POTENTIAL ENERGY BARRIERS TO ION TRANSPORT WITHIN LIPID BILAYERS

STUDIES WITH TETRAPHENYLBORATE

OLAF SPARRE ANDERSEN *and* MARTIN FUCHS

From the Departments of Physiology and Biophysics, Cornell University Medical College, New York 10021

ABSTRACT Tetraphenylborate-induced current transients were studied in lipid bilayers formed from bacterial phosphatidylethanolamine in decane. This ion movement was essentially confined to the membrane interior during the current transients. Charge movement through the interior of the membrane during the current transients was studied as a function of the applied potential. The transferred charge approached an upper limit with increasing potential, which is interpreted to be the amount of charge due to tetraphenylborate ions absorbed into the boundary regions of the bilayer. A further analysis of the charge transfer as a function of potential indicates that the movement of tetraphenylborate ions is only influenced by a certain fraction of the applied potential. For bacterial phosphatidylethanolamine bilayers the effective potential is $77 \pm 4\%$ of the applied potential. The initial conductance and the time constant of the current transients were studied as a function of the applied potential using a Nernst-Planck electrodiffusion regime. It was found that an image-force potential energy barrier gave a good prediction of the observed behavior, provided that the *effective potential* was used in the calculations. We could not get a satisfactory prediction of the observed behavior with an Eyring rate theory model or a trapezoidal potential energy barrier.

INTRODUCTION

The basic mechanisms of ion transport through phospholipid (bilayer) membranes are understood along fairly general lines (18). It is established that the major contribution to the barrier properties of these membranes is the large electrostatic charging energy, or work, (primarily the Born energy due to the difference in dielectric constants) necessary to move an ion out of an aqueous phase into the hydrocarbon phase in the membrane interior (12). The magnitude of this work decreases with increasing size of the ion (6, 12). Membrane permeable ions are therefore large organic ions, e.g. tetraphenylborate or tetraphenylarsonium, or complexes of small inorganic ions with ion carriers, e.g., K^+-nonactin, K^+-valinomycin. This electrostatic work, or energy requirement, is not constant through the membrane, but is modified by attractive forces between the ion within the membrane and the aqueous phases (18, 21, 29, 38).

The charging energy is only one component of the total potential energy of an ion, or

ion-ion carrier complex, within the bilayer. Other components are hydrophobic interactions between the ion and the aqueous phases (49), electrostatic potential differences (both surface and dipole potentials) between the membrane interior and the bulk aqueous phases (19, 31–33, 35, 48), and short range (packing) interactions between the ion and molecules in the bilayer. The sum of these four terms constitutes the potential energy barrier to ion transport through the membrane. The potential energy of an ion within the membrane may also be affected by an applied potential difference. This is, however, not a part of the potential energy barrier. Ion transport through the membrane, and its dependence on the applied potential, is determined by the shape of the potential energy barrier through the bilayer (4, 7, 17, 18, 20, 21, 23, 27–29, 38, 46, 47). All four terms in the potential energy barrier are of importance in determining the magnitude of the membrane permeability (conductance). The potential dependence of ion transport through the middle of the membrane will be determined by the electrostatic charging energy term (21, 29, 38), because it is the only term which changes significantly through the entire membrane. Any of the four terms, as well as other terms (ion-ion carrier association and dissociation kinetics), may be of importance if the current-carrying species cross the membrane-solution interfaces.

If one knows the shape of the potential energy barrier for a current-carrying species, one may calculate the current-voltage characteristics of the membrane in the presence of this species (7, 17, 18, 20, 21, 23, 29, 38). Deviations between experiment and simple predictions are used to obtain information about the kinetics of ion-ion carrier association and dissociation reactions (4, 7, 20, 21, 27, 28, 46, 47). In principle it is also possible to perform the inverse operation and obtain information about the shape of the potential energy barrier in the middle of the membrane from an analysis of experimental current-voltage characteristics (17, 21). However, if the current-carrying species used in such a study is actually crossing the membrane-solution interfaces the arguments become circular, since one cannot separate phenomena due to the interfacial "barrier" from phenomena due to the barrier in the middle of the membrane. The interpretation of experimental current-voltage characteristics will therefore be dependent upon simplifying assumptions about what happens at the membrane-solution interfaces. A further experimental limitation is the fact that one can only study current-voltage characteristics over a limited range of applied potentials. An infinite number of possible potential energy barrier shapes will therefore be able to explain any observed current-voltage characteristics. Consequently, there are divergent reports about the "correct" shape of the potential energy barrier to ion transport in the center of lipid bilayers (4, 17, 21, 23).

An additional, but often overlooked, problem is that ion transport through membranes should be related to the *effective potential* influencing ion movement within the membrane, not to the applied potential. An analysis of experimental current-voltage characteristics of lipid bilayers to obtain information about the shape of the potential energy barrier therefore depends on an independent determination of the effective potential.

One possible method to circumvent some of these problems is to use current carriers that do not cross the membrane-solution interfaces to any significant extent, once the membrane is loaded. Certain organic anions, e.g. tetraphenylborate, absorb strongly into the membrane-solution boundary regions (23, 30, 32). These ions will therefore provide information about the shape of the potential energy barrier in the middle of the membrane, independent of assumptions about what happens at the membrane-solution interfaces. There should be little, if any, difference between the movement of an organic ion and an ion-ion carrier complex through the interior of a lipid bilayer. This system, therefore, serves as a simple model for the transport of ion-ion carrier complexes through these membranes. In addition, it may serve as a model for some properties of the "gating currents" observed in excitable membranes (2, 24).

In preliminary experiments it was found that the kinetics of tetraphenylborate transport through lipid bilayer could not be quantitatively described by the assumption of a single Eyring-type barrier, a model developed by Ketterer et al. (23). The aim of the present investigation, therefore, was to study experimentally the shape of the potential energy barrier in the middle of the membrane. Tetraphenylborate is very suitable to this purpose since it absorbs so strongly into the bilayer that one can *measure the number of ions absorbed into the boundary regions of the bilayer* independent of any particular kinetic model for the transport mechanism. Using this property, we can show that only a certain fraction (<1) of the applied potential is effective in moving these ions through the membrane. Using this information we can show that the potential energy barrier to ion transport through the center of the bilayer is closely related to the image-force barrier of Neumcke and Läuger (29, 38).

THEORY

To a first approximation a lipid bilayer can be treated as a thin slab of hydrocarbon having a thickness, d, of 25–50 Å and a dielectric constant, ϵ_m, approximately 2, between two aqueous phases with a dielectric constant, ϵ_{H_2O}, approximately 80. We shall assume that only one charged species (current carrier) is present within the membrane, in our case tetraphenylborate ($TPhB^-$). NaTPhB is present in equal concentrations in the aqueous phases on both sides of the membrane. An excess of an inert electrolyte, NaCl, is also present in the aqueous phases, to maintain the ionic strength constant, independent of the concentration of NaTPhB, and to ensure a high conductance of the aqueous phases compared with the membrane. The $TPhB^-$ ions will absorb very strongly into the membrane-solution boundary regions, while the Na^+ (and Cl^-) ions will stay behind in the aqueous phases, and thus will not be able to carry current through the membrane.

The potential energy barrier, $W(x)$, to ion transport through the membrane is shown in Fig. 1 A. The potential energy of an ion in the bulk aqueous phases is assumed constant equal to zero. $W(x)$ will begin to change when the center of the ion is located a distance of one ion radius, r, from the membrane-solution interfaces. The sum of the four terms making up $W(x)$ has a deep, narrow, minimum near the two interfaces,

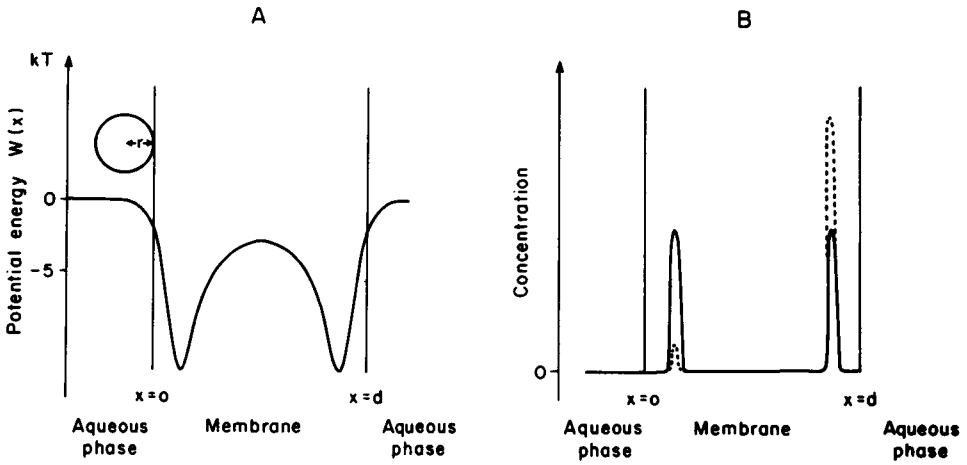

FIGURE 1 (*A*) Schematic representation of the potential energy barrier to ion transport across a bimolecular lipid membrane. Curve drawn according to the data obtained in the present article. (*B*) Schematic representation of concentration profile for $TPhB^-$ within the bilayer. The full line is drawn for a potential difference of 0 mV, the stippled line is drawn for a potential difference of about 75 mV.

which are separated by a broad barrier in the center of the membrane due to the electrostatic charging energy, $W_e(x)$.[1] The occurrence of these potential energy minima within the membrane, near the two interfaces, is characteristic for large hydrophobic ions (23) and ion-ion carrier complexes.

Thus $TPhB^-$ ions absorbed into the membrane will be concentrated in two very narrow strips located near, but not necessarily at, the two membrane-solutions interfaces, see Fig. 1 B. When an electrical potential difference is applied across the membrane this will lower the potential energy of the ions in one of the minima compared to the other (the positive). Consequently the $TPhB^-$ ions within the membrane will tend to accumulate into the "positive" minimum (see Fig. 1 B) and thus give rise to a current through the membrane.

Since the ions absorbed into the membrane are located in two quite narrow strips one can assume that the *number* of ions N_I and N_{II} per unit area present in the energy minima is proportional to the *concentrations* of ions at the minima, C_I and C_{II} (18).

$$N_I = \gamma \cdot C_I, \tag{1 A}$$

$$N_{II} = \gamma \cdot C_{II}, \tag{1 B}$$

where the subscripts I and II denote the left and right boundary region, respectively,

[1]The electrostatic potential difference between membrane interior and bulk aqueous phases is usually positive (19), which will tend to favor the distribution of anions into the membrane over cations. On the other hand, the hydration energy for cations is (numerically) less than for anions (6), which will tend to favor the distribution of cations into the membrane over anions. The potential energy barrier is therefore qualitatively the same for both anions and cations.

and γ represents the volume per unit membrane area into which the absorbed ions are concentrated. The existence of these potential energy minima, and consequent concentration peaks, is an essential assumption of the model which is outlined below.

Charge Movement through the Membrane

At a time $t = 0$ a potential difference, V, is suddenly applied across the membrane. $TPhB^-$ ions will move through the membrane, and the ion concentration within the membrane will shift from the equilibrium profile to some new profile which will be a function of V (and time). The time course of the concentration changes will be given by the continuity equation

$$\partial j/\partial x = -\partial C/\partial t, \tag{2}$$

where $j(x,t)$ denote the flux of $TPhB^-$ which may be a function of distance, $x(x = 0$ at one and $x = d$ at the other membrane-solution interface), and time, t; $C(x,t)$ denote the concentration of the ions in the membrane and adjoining aqueous phases. We assume that for $t < 0$, $C(-r)$ and $C(d + r)$ are equal to the bulk concentration, C_{Aq}, of $TPhB^-$ in the aqueous phases. It should be recalled that r is the contact distance of the ion center to the membrane-solution interfaces.

We may integrate Eq. 2 from $x = -r$ to $x = d/2$ and obtain

$$j\left(\frac{d}{2}, t\right) - j(-r,t) = -\int_{-r}^{d/2} \frac{\partial c}{\partial t}\, dx. \tag{3}$$

Stated differently, the net flux of $TPhB^-$ ions through the membrane, $j[(d/2), t]$, is equal to the net flux into the membrane, $j(-r, t)$, plus the rate of decrease in the number of absorbed ions $-\int_{-r}^{d/2} (\partial c/\partial t)\, dx$. One can further integrate Eq. 3 with respect to time and obtain

$$\int_0^t j\left(\frac{d}{2}, \zeta\right) d\zeta - \int_0^t j(-r,\zeta)\, d\zeta = -\int_{-r}^{d/2} (C(x,t) - C(x,0)\, dx, \tag{4}$$

where ζ is an integration variable.

Eq. 4 states that the integrated charge movement through the membrane is equal to the net entry of ions into the membrane plus the net change in the number of absorbed ions. It is possible (see ref. 11, section 3.3)[2] to obtain an upper estimate for

$$\int_0^t j(-r,\zeta)\, d\zeta \leq 2AC_{Aq}(Dt/\pi)^{1/2}, \tag{5}$$

[2]The estimate in Eq. 5 is valid *both* for diffusional entry of $TPhB^-$ ions into the membrane, as well as for diffusional exit of $TPhB^-$ into the aqueous phases. The calculation assumes that the membrane-solution interface does not form a barrier to ion movement, and that the concentration of $TPhB^-$ within the membrane is maintained at zero, or two times the equilibrium boundary region concentration, respectively. The rate-limiting step for ion movement across the interfaces is diffusion in the aqueous phases.

where D denotes the diffusion coefficient of $TPhB^-$ in the aqueous phases, 5.3×10^{-6} cm^2/s (44), and A, 1.3 mm^2, is the membrane area. If $C_{Aq} = 10^{-7}$ M one obtains after 10 ms

$$\int_0^t j(-r,\zeta)\, d\zeta \leq 3 \times 10^{-16} \text{ mol.}$$

Experimentally we know that 4×10^{-15} mol of $TPhB^-$ can move through bacterial phosphatidylethanolamine bilayers in less than 10 ms (see Results) so that at most 8% of the net ion flux through the center of the membrane is due to ion movement across the membrane-solution interfaces. It should be noted that this argument is independent of any assumption about the relative resistances of the membrane-solution interface and the membrane interior, respectively (see also ref. 18). The actual exchange of ions across the membrane-solution interfaces will be less than these estimated upper limits. We conclude that so many $TPhB^-$ ions absorb into the membrane-solution boundary regions (in a potential energy minimum) that it is possible to disregard any ion transport across the interfaces compared with ion transport through the membrane so that the number of ions absorbed into the membrane is constant, $N_I + N_{II}$ = constant. This has three consequences: Firstly, the current through the interior of the bilayer will be carried by $TPhB^-$ (at least in all cases of interest to us) while current passing across the interfaces will be a displacement current. Secondly, the current through the membrane cannot be maintained at the initially "high" level, but will relax towards a very low level (see Fig. 2) which is determined by the transport of $TPhB^-$ across the interfaces and through the aqueous phases adjacent to the membrane.[3] Thirdly, one boundary region will become depleted of $TPhB^-$ while the other will accumulate $TPhB^-$ ions (see Fig. 1 B).

When no current is flowing across the membrane, one can calculate the relative concentrations of $TPhB^-$ in the two boundary regions using the Boltzmann distribution

$$C_I \cdot \exp(-zq\phi_I/kT) = C_{II} \cdot \exp(-zq\phi_{II}/kT) \tag{6}$$

where C_I is the concentration of $TPhB^-$ in the potential energy minimum near $x = 0$, ϕ_I is the electrostatic potential at the minimum due to the applied potential V, C_{II} and ϕ_{II} are the corresponding quantities near $x = d$, z is valency, q is the protonic charge, k is Boltzmann's constant, T is temperature in degrees Kelvin, x is distance through the bilayer from left to right. The number of ions transported through the center of the membrane $\Delta N(V)$ can be expressed as

$$\Delta N(V) = [(N_{Abs} + \Delta N(V)) - (N_{Abs} - \Delta N(V))]/2 = (N_{II} - N_I)/2, \tag{7}$$

where N_{Abs} is the total number of ions absorbed into one boundary region of the membrane. Combining Eqs. 1 A, B, 6, and 7 with $N_I + N_{II} = 2N_{Abs}$ we obtain that

[3] If the membrane-solution interfaces were ideal boundaries the current would decline to zero.

$$\Delta N(V) = N_{Abs} \cdot \tanh(-qz(\phi_{II} - \phi_I)/2KT). \quad (8)$$

We have assumed that the energy minima are deep and narrow, so their positions are independent of the applied potential, and we may put

$$\phi_{II} - \phi_I = \beta \cdot V, \quad (9)$$

where β is the fraction of the applied potential that is actually effective in moving ions through the membrane. Combining Eqs. 8 and 9 and setting $z = -1$ we obtain

$$\Delta N(V) = N_{Abs} \cdot \tanh(\beta qV/2kT). \quad (10)$$

From Eq. 10 it can be seen that the number of ions moved through the membrane during a current transient reaches an upper limit, N_{Abs}, with increasing potential.[4] Experimentally one can therefore determine both N_{Abs} and β by studying $\Delta N(V)$ as a function of V. This determination of N_{Abs} and β is independent of any particular shape of the potential energy barrier to ion transport within the bilayer. This demonstrates the fairly unique properties of $TPhB^-$ as a tool to study ion transport within membranes, because a model-independent knowledge of β constitutes a critical step in the analysis of the shape of the potential energy barrier.

Kinetics of the Current Relaxations

Ion transport through a lipid bilayer may be described by the Nernst-Planck electrodiffusion equations (39) provided one includes a term to describe variations in the potential energy barrier through the membrane (25, 29, 38).

Since we are measuring current-*transients*,

$$(\partial C/\partial t) = A(\partial/\partial x)\{u(x)[kT(\partial C/\partial x) + zq \cdot C(x,t)(\partial\phi/\partial x) + C(x,t)(\partial W/\partial x)]\}, \quad (11)$$

where $u(x)$ is the mobility of the current-carrying species ($TPhB^-$) within the membrane, $\phi(x)$ is the electrostatic potential due to an externally applied potential, which must be clearly distinguished from $W(x)$ which is the inherent potential energy barrier within the membrane. Even though concentration profiles and ion flux change with time, one can regard the transport process to be pseudo-stationary if the charging time constant τ_C, (the time constant for changes of concentration profiles in the *center* of the bilayer at $t = 0$), is much smaller than the time constant τ, of the observed current transient (39). In Appendix I we show that τ_C is approximately 2 μs while we experimentally restrict ourselves to $\tau > 200$ μs. We can, therefore, following Planck (39), integrate Eq. 11 via the continuity equation to obtain, setting $z = -1$,

$$j = -A \cdot u(x) \cdot [kT(dC/dx) - C(x,t) \cdot q(d\phi/dx) + C(x,t)(dW/dx)], \quad (12)$$

[4]For small applied potentials, $V < kT/q$, Eq. 10 becomes similar to the usual condenser equation $Q = CV$, where Q is charge and C is capacitance.

where j is the flux of ions. Eq. 12 is similar to the usual form of the Nernst-Planck equations. It should be emphasized that Eq. 12 is only valid some time ($\sim 10\ \mu s$) after applying a potential difference across the membrane. For practical purposes one may, however, assume that Eq. 12 is valid for all times after applying the potential.

Eq. 12 may be integrated to give

$$j(V,t) = \frac{-AkT[C_{II} \cdot \exp(-\beta qV/2kT) - C_I \cdot \exp(\beta qV/2kT)]}{\exp(qV/2kT) \int_{\eta}^{d-\eta} [1/u(x)] \cdot \exp([W_1(x) - q\phi(x)]/kT)\, dX}, \quad (13)$$

where η denotes the distance of the energy minima from the interfaces, and $W_1(x) = W(x) - W(\eta)$. The exponential function in the integral varies by several orders of magnitude, thus variations in $u(x)$ are of small consequence for the behavior of the integral in Eq. 13. We may therefore assume the ion mobility to be independent of position $u(x) = u$.

The current through the membrane, $I(V,t)$, is defined as $I(V,t) = qj(V,t)$ (note the sign convention). The membrane conductance, $g_m(V,t)$, is usually defined as

$$g_m(V,t) = I(V,t)/[V - E(t)], \quad (14\,A)$$

where $E(t)$ denotes electromotive force which will be a function of time

$$E(t) = (kT/q) \cdot \ln [C_{II}(t)/C_I(t)].$$

The electromotive force as defined above is a measure of polarization *within* the membrane, and can in general not be measured with external electrodes in the aqueous phases, whereas the electrical potential difference, V, is measured *across* the entire membrane. The existence of such a membrane polarization or diffusion potential is a consequence of our assumption concerning the potential energy minima near the two membrane-solution interfaces. $E(t)$ may therefore be regarded as a diffusion potential between the two potential energy minima within the membrane, thus emphasizing the difference between ion transport within the membrane compared with current flow across the membrane when $\beta < 1$. It is consequently advantageous to define a barrier conductance, $g_b(V,t)$, as

$$g_b(V,t) = I(V,t)/[\beta \cdot V - E(t)], \quad (14\,B)$$

where $\beta \cdot V$ is the actual electrical potential difference influencing ion movement within the membrane.

By substituting Eq. 13 into Eq. 14 B we obtain the general expression for the barrier conductance

$$g_b(V,t) =$$

$$\frac{-AkTqu[C_{II}\cdot\exp(-\beta qV/2kT) - C_I\cdot\exp(\beta qV/2kT)]}{[\beta V - (kT/q)\cdot\ln(C_{II}/C_I)]\cdot\exp(qV/2kT)\cdot\int_{\eta}^{d-\eta}\exp([W_1(x) - q\phi(x)]/kT)} \quad (15\,A)$$

One can compare Eq. 15 A with the classical Nernst-Planck expression for membrane conductance, $g(V,t)$,

$$g(V,t) = \frac{A}{\int_{\eta}^{d-\eta} dx/[uq^2C(x,t)]}, \quad (15\,B)$$

see, for example, ref. 13. We can thus emphasize the difference between g_m and g_b, because $g(V,t) = g_b(V,t)$ (see Appendix II), while $g(V,t) \neq g_m(V,t)$ when $\beta < 1$.

At $t = 0$, $C_I = C_{II} = C$, and $E(0) = 0$, so the initial current is

$$I(V,0) = \frac{AukTqC2\cdot\sinh(\beta qV/2kT)}{\exp(qV/2kT)\int_{\eta}^{d-\eta}\exp([W_1(x) - q\phi(x)]/kT)\,dx}, \quad (16)$$

while the initial membrane conductance, $g_m(V,0)$, is obtained as

$$g_m(V,0) = \frac{I(V,0)}{V} = \frac{AukTqC2\cdot\sinh(\beta qV/2kT)}{V\cdot\exp(qV/2kT)\int_{\eta}^{d-\eta}\exp([W_1(x) - q\phi(x)]/kT)\,dx}. \quad (17)$$

However, we are really interested in the initial barrier conductance, $g_b(V,0)$, because it is this latter quantity that describes ion movement within the membrane. But the normalized initial conductance is

$$g_m(V,0)/g_m(0,0) = [I(V,0)/V]/\lim_{V\to 0}\{I(V,0)/V\}$$

$$= [I(V,0)/\beta V]/\lim_{V\to 0}\{I(V,0)/\beta V\} = g_b(V,0)/g_b(0,0), \quad (18)$$

where $g_m(0,0)$ and $g_b(0,0)$ denote the initial small signal (ohmic) membrane and barrier conductance, respectively. It is thus necessary to use the normalized initial conductance when analyzing the current-voltage characteristics to obtain information about ion movements in the membrane interior.

The time course of the current transients may be calculated using the assumption

that all ions absorbed into the bilayer are located into the two boundary regions. Ion movement through the membrane interior can therefore be described as

$$N_{\mathrm{I}}(t) = N_{\mathrm{Abs}} - \frac{1}{A} \cdot \int_0^t j(V, \zeta)\, \mathrm{d}\zeta, \tag{19 A}$$

$$N_{\mathrm{II}}(t) = N_{\mathrm{Abs}} + \frac{1}{A} \cdot \int_0^t j(V, \zeta)\, \mathrm{d}\zeta. \tag{19 B}$$

We may substitute Eqs. 1 A, 1 B, 19 A, 19 B into Eq. 13 to obtain

$$j(V,t) = \frac{-AukT}{\gamma \cdot \exp(qV/2kT) \int_{\eta}^{d-\eta} \exp([W_1(x) - q\phi(x)]/kT)\, \mathrm{d}x} \times \left\{\left(N_{\mathrm{Abs}} + \frac{1}{A} \cdot \int_0^t j(V,\zeta)\, \mathrm{d}\zeta\right) \cdot \exp(-q\beta V/2kT) - \left(N_{\mathrm{Abs}} - \frac{1}{A}\int_0^t j(V,\zeta)\, \mathrm{d}\zeta\right) \cdot \exp(q\beta V/2kT)\right\}, \tag{20}$$

or

$$\mathrm{d}j/\mathrm{d}t = -j(V,t) \cdot \frac{ukT2 \cdot \cosh(\beta qV/2kT)}{\gamma \cdot \exp(qV/2kT) \int_{\eta}^{d-\eta} \exp([W_1(x) - q\phi(x)]/kT)\, \mathrm{d}x},$$

or

$$I(V,t) = I(V,0) \cdot e^{-t/\tau(V)}, \tag{21}$$

where

$$\tau(V) = \frac{\gamma \cdot \exp(qV/2kT) \int_{\eta}^{d-\eta} \exp([W_1(x) - q\phi(x)]/kT)\, \mathrm{d}x}{ukT2 \cdot \cosh(q\beta V/2kT)}. \tag{22}$$

It is apparent that both current vs. voltage and time constant vs. voltage behavior will be dependent on the behavior of $f(V)$, where

$$f(V) = \exp(qV/2kT) \int_{\eta}^{d-\eta} \exp([W_1(x) - q\phi(x)]/kT)\, \mathrm{d}x. \tag{23}$$

An integration of the integral in Eq. 23 demands information about the behavior of both $W_1(x)$ and $\phi(x)$ through the membrane. The experiments are done under con-

ditions where the free space charge (concentration of $TPhB^-$) in the interior of the membrane is very low ($<10^{-5}$ M) so one may assume that $\phi(x)$ varies linearly through the membrane (29).[5] The major variation in $W_1(x)$ is the electrostatic interactions between an ion within the membrane and the aqueous phases. A useful approximation for $W_1(x)$, apart from an additive constant, will therefore be the electrostatic charging energy, $W_e(x)$. In Appendix III we have calculated $W_e(x)$ assuming the aqueous phases to be perfect conductors and the $TPhB^-$ ions to be ideally nonpolarizable, so that they may be treated as point charges. The integral in expression 23 was evaluated numerically. The final result is that

$$f(V) = \exp(qV/2kT) \int_{\P}^{d-\P} \exp([W_e(x) - q\phi(x)]/kT)\,dx$$

$$= \exp[\omega \cdot (qV/kT)^2] \int_{\P}^{d-\P} \exp(W_e(x)/kT)\,dx, \qquad (24)$$

where ω is a parameter dependent on membrane thickness (see also ref. 18) which is tabulated in Table I, p. 813. The analytical form for $W_e(x)$, or $W_1(x)$, does not enter explicitly into Eq. 24, but it can rather easily be seen (see the Discussion section and Appendix III) that the analytical expression for the potential dependent behavior, the function $F(V)$,

$$F(V) = f(V)/f(0) = \exp[\omega(qV/kT)^2], \qquad (25)$$

is dependent on the analytical expression for the potential energy barrier. The potential dependence of $f(V)$ is therefore given by $F(V)$ which in principle also contains all information about the shape of the potential energy barrier.

From Eqs. 16 and 21 it can be seen that "immediately" after the application of a potential difference across the membrane an initial current $I(V,0)$ will flow, which is due to a redistribution of ions between the two boundary phases. The current decays exponentially toward a stationary value, ideally zero. The reason for the decay is polarization with the membrane, causing a back diffusion of ions thus diminishing the net current. At the end of the stimulus, one will observe a new current transient in opposite direction, since one will have $V = 0$ but $C_{II} \neq C_I$ in Eq. 13. By repeating the previous analysis with $t = 0$ when the potential returns from V to zero, one obtains

$$I_{V,t}(0,0) = -AukTq(C_{II} - C_I) / \int_{\P}^{d-\P} \exp(W_1(x)/kT)\,dx, \qquad (26)$$

$$g_{V,t}(0,0) = AukTq(C_{II} - C_I) / \left(E_{V,t}(0,0) \int_{\P}^{d-\P} \exp(W_1(x)/kT)\,dx\right), \qquad (27)$$

[5] The estimate obtained by Läuger and Neumcke (29) is obtained for membranes with a horizontal potential energy profile (no barrier) but should be valid as an order of magnitude estimate.

$$\tau(0) = \left(\gamma \int_{\eta}^{d-\eta} \exp(W_1(x)/kT)\,dx\right)/2ukT, \qquad (28)$$

where $I_{V,t}(0,0)$ is the initial current when the potential returns from V to zero and the potential was on for t ms; $g_{V,t}(0,0)$ signifies the corresponding initial conductance (barrier conductance), $\tau(0)$ is the time constant for the "off" current relaxation and $E_{V,t}(0,0)$ is the corresponding electromotive force due to the membrane polarization. For $t \gg \tau$, $E_{V,t}(0,0) = \beta \cdot V$. The existence of this back-diffusion of ions shows that the main cause of the current decline with time is the buildup of an electromotive force within the membrane. Conductance changes do, however, play a role in the decrease of current with time. Conductance changes occur instantaneously upon potential changes, disregarding the first few microseconds. The range of variation of conductances is therefore most easily estimated from the initial conductances for the back-diffusion current transients.

METHODS AND MATERIALS

Bimolecular lipid membranes were formed at room temperature (24–26°C) by the brush technique of Mueller et al. (34) across a hole, 1.5 mm^2 area, in a Teflon partition separating two Teflon chambers containing symmetrical unbuffered 0.1 M NaCl solutions. In most experiments reported here the membrane forming solution was bacterial phosphatidylethanolamine dissolved in *n*-decane, 2.5% wt/vol. Some experiments were done with dioleoylphosphatidylethanolamine in *n*-decane. After the membrane was formed, small aliquots of NaTPhB were added to both aqueous phases under continuous stirring. The membrane conductance reached a steady level within a few (<5) minutes. After completion of one set of measurements, a further addition of NaTPhB was made and the measurements repeated, etc. NaTPhB was dissolved in both ethanol and 0.1 M NaCl with no change in results. In view of the instability of NaTPhB in aqueous solutions, the aqueous solutions were made up fresh every day while the ethanolic solutions were stock solutions. Control experiments showed that 2.5% ethanol (vol/vol) changes membrane conductance and relaxation time constant by less than 20%. In no case did we use ethanol concentrations higher than 1.0%.

The electrical measurements were performed with a two-electrode "voltage clamp." A potential difference, V, could be applied across the membrane by a function generator with a rise time of about 2 μs, and an internal resistance of <10 Ω. Except in a few preliminary experiments where calomel electrodes were used, the electrodes were Ag/AgCl electrodes with a surface area of 2.5 cm^2. The total series resistance to the membrane was 800–1,000 Ω. The membrane capacitance is about 8×10^{-9} F (membrane area $\sim$1.3 mm^2), so the charging time of the membrane is $\sim$8 μs. Membrane current was measured with a fast-settling, high slew rate, differential amplifier. To eliminate overloading, and increase response time of the amplifier at high gains, a voltage-limiting filter was built into the feedback loop. The time constant of the current measuring amplifier varied from <1 μs to 5 μs. The effective time resolution of the total system is, therefore, around 100 μs. A few experiments were done with a three electrode system to check that the system did actually "clamp" the membrane properly.

To check the electrical measuring system, and to exclude that electrode polarization played any role in the observed current relaxations, we tested the response with "dummy" equivalent circuits similar to the procedure of Ketterer et al. (23).

The time course of the current relaxations was recorded on a storage oscilloscope and photographed for later analysis. The analysis was initially performed by hand, but was later

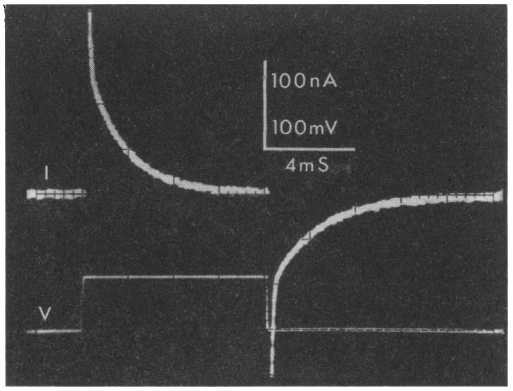

FIGURE 2 An oscillogram of $TPhB^-$ current transient in a BPE-decane membrane. The top trace shows current, the lower trace potential as a function of time. Stimulus 60 mV, duration 8 ms. The aqueous phases contained 0.1 M NaCl and 7×10^{-8} M tetraphenylborate, membrane area 1.2 mm^2. T = 25°C.

done on a programmable calculator. Bacterial phosphatidylethanolamine was obtained from Supelco, Inc., Bellefonte, Pa. Dioleoylphosphatidylethanolamine was a gift from Dr. P. Läuger, Konstanz. *n*-Decane (gas chromatographic standard) and NaTPhB were obtained from EM Laboratories, Inc., Elmsford, N.Y. NaCl was analytical grade. High purity deionized water, Continental or Millipore Milli "Q," was used throughout the experiments.

RESULTS

Charge Movement across Lipid Bilayers in the Presence of Tetraphenylborate

A typical example of current relaxations in the presence of $TPhB^-$ is seen in Fig. 2. The current, $I(t)$, is shown as a function of time after a stimulus with an amplitude V = 60 mV and a duration of 8 ms. The aqueous solution contained 7×10^{-8} M NaTPhB and 0.1 M NaCl. After an initial very fast current transient (not seen fully in the photograph) which charges the membrane capacitance, the current through the membrane declines with a time constant, τ, of about 1.4 ms ("on" response). At the end of the stimulus the membrane capacitance discharges and one observes a current relaxation, of opposite polarity to the first, with a time constant of about 2.0 ms ("off" response). The initial current, $I(0)$, is obtained by plotting log $I(t)$ vs. time and extrapolating the "slow" transient back to $t = 0$. The initial conductance of the "on" response is calculated using Eq. 14 A with $E(0) = 0$. As can be seen in Fig. 3, the "slow" current relaxations are, indeed, exponential for more than three time constants, indicating that only a few percent of the ions have moved across the two membrane-solution interfaces during the current transients. The records were usually analyzed for more than one time constant. A log-linear regression was performed, and the correlation coefficients were better than 0.99, in many cases, 0.999. It was checked that the calculated $I(0)$ was similar to $I(0)$ read off the photograph.

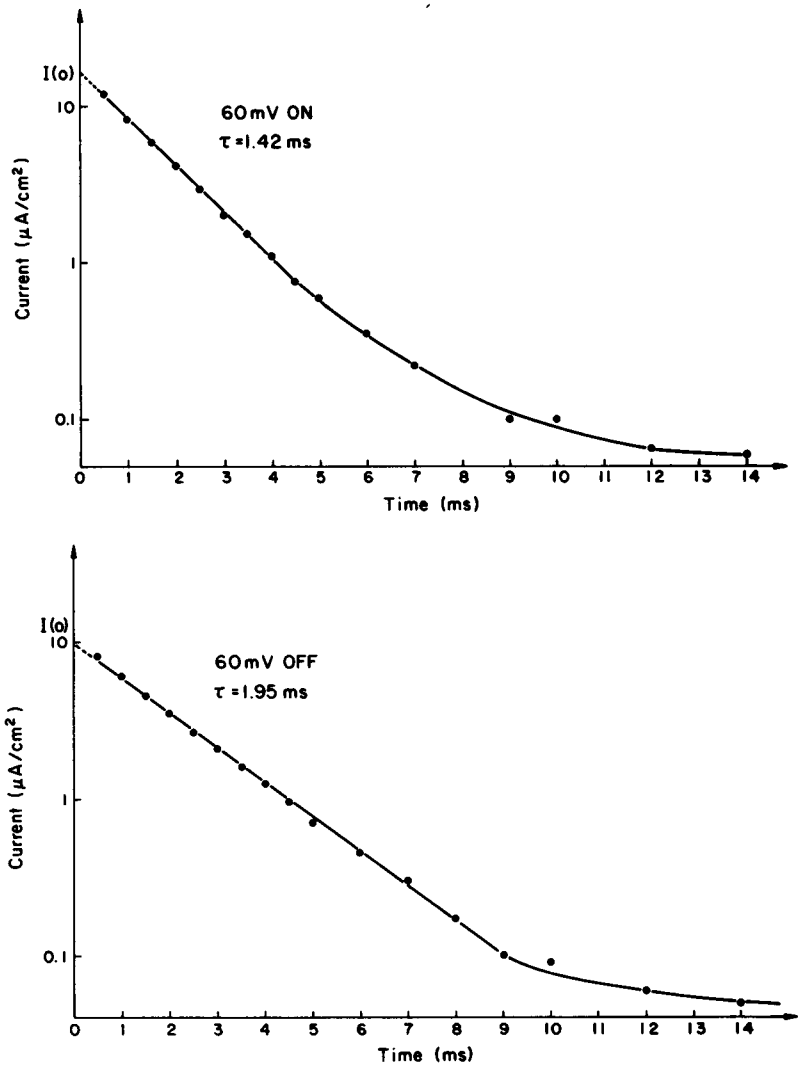

FIGURE 3 *Top* (*A*): Plot of log current vs. time for an "on" response. *Bottom* (*B*): Plot of log current vs. time for an "off" response. Both plots were obtained by analyzing several pictures obtained on the same membrane. The aqueous phases contained 0.1 M NaCl and 7×10^{-8} M tetraphenylborate. $T = 25°C$.

If the ion movements were confined to the membrane, the current would continue its exponential course towards $I = 0$. A small but finite ion transport occurs across the membrane-solution interfaces (see Fig. 3 A and B). The magnitude of this current is mainly determined by diffusion polarization in the aqueous phases, consistent with the fact that the current traces in Fig. 3 A and B are superimposable for $t > 9$ ms.

The deviations from linearity in Fig. 3 A were analyzed further. It was found that they had a time course consistent with diffusional transport of $TPhB^-$ ions in the

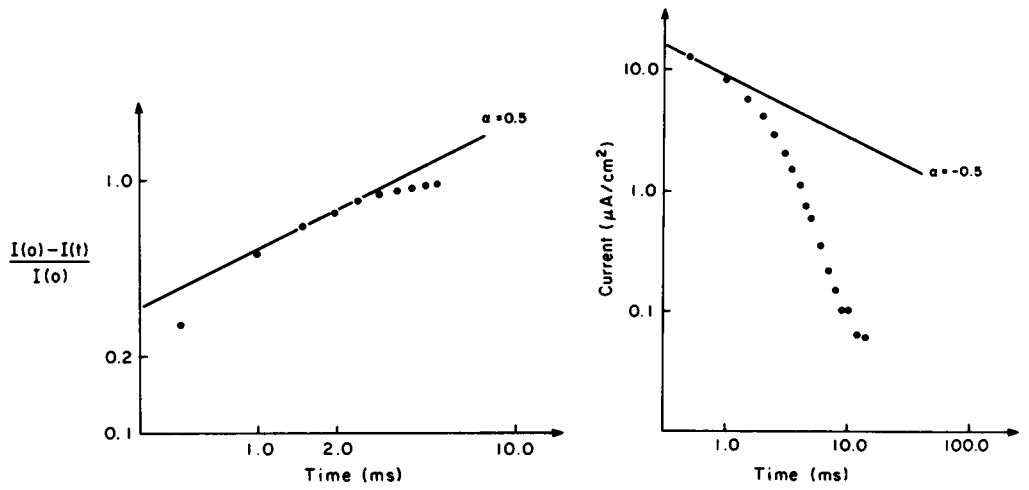

FIGURE 4 Test for aqueous diffusion polarization. *Left:* Plot of log $[(I(0) - I(t))/I(0)]$ vs. log t, should give a straight line with a slope of 0.5 if aqueous diffusion polarization is a significant factor in determining the time course of the current transient for "short" time intervals. *Right:* Plot of log $I(t)$ vs. log t, should give a straight line with a slope of −0.5 if aqueous diffusion polarization is a significant factor in determining the time source of the current transient for "long" intervals. Experiment from Fig. 3 A.

aqueous phases up the membrane, and that about 5% of the ions moved through the center of the membrane had actually crossed the membrane-solution interfaces.

If the observed current relaxations were mainly due to diffusion polarization in the aqueous phases the current would be described by the following expression (37): $I(t) = I(0) \cdot \exp(Dt/\alpha_N^2) \cdot \operatorname{erfc}(dt/\alpha_N)$ where α_N is a composite parameter (see ref. 37), and erfc is the error-function complement (1, 11). For small values of t this expression is approximated by $(I(0) - I(t))/I(0) \sim \sqrt{t}$, whereas for large values of t the approximation is $I(t) \sim 1/\sqrt{t}$ (37).

The experimentally observed shape of the current relaxation may, therefore, be used to distinguish between a transport mechanism dominated by internal membrane polarization or by diffusion polarization in the aqueous phases. In Fig. 4 we have plotted the experimental data from Fig. 3 A to test whether diffusion polarization in the aqueous phases plays any significant role in determining the time course of the current transient for either small or large t. A comparison with Fig. 3 A shows that the time course of the current is inconsistent with such a mechanism playing any major role.

It should be noted that at small applied potentials the current relaxations may appear exponential even when diffusion polarization plays a major role in determining the time course of the current transients. The "time constant" for these transients is, however, anomalously high, and an analysis of the current relaxations at higher applied potentials will show definite diffusion polarization behavior.

The number of coulombs moved through the bilayer during a single current transient given by $\int_0^\infty I(t)\,dt$ which, in our case, may be approximated by

$$\int_0^\infty I(0) \cdot e^{-t/\tau} dt = I(0) \cdot \tau. \quad (29)$$

In Fig. 5 we have plotted $I(0) \cdot \tau$ vs. the applied potential. It is apparent that the charge moved through the membrane reaches an upper limit with increasing potential. This upper limit, which we interpret to be $q \cdot N_{Abs}$, corresponds to the complete depletion of $TPhB^-$ ions in one boundary region in Fig. 1 B. Fig. 5 also demonstrates that the charge moved through the bilayer during the on-response is exactly matched by charge moving back during the off-response.

The decline in current with time should, according to the model, be due to a charge accumulation in one boundary phase (the positive) and a corresponding depletion in the other. The time constant for the charge accumulation should be identical to that for the current transient itself. The charge accumulated at time t, $C(t)$ is described by $C(\infty) \cdot (1 - e^{-t/\tau})$, where τ is the time constant of the on-response and $C(\infty) = I(0) \cdot \tau$. In Fig. 6 we have plotted log $(C(\infty) - C(t))$ vs. t, and obtained a straight line with $\tau = 1.30$ ms. τ for the on-response is 1.35 ms. We therefore conclude that the observed current relaxations are mainly due to charge redistributions *within* the bilayer and only secondarily to membrane conductance changes. Consequently one may use

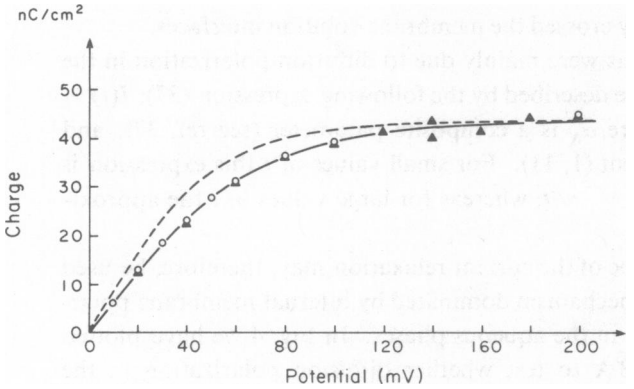

FIGURE 5

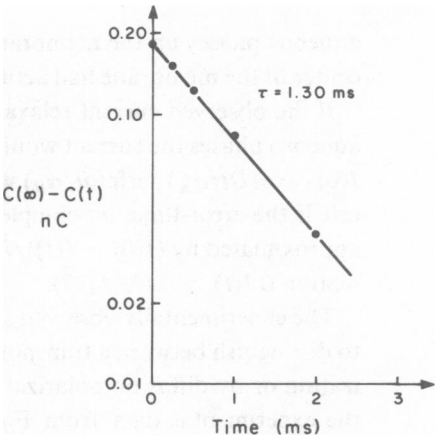

FIGURE 6

FIGURE 5 Plot of $I(0) \cdot \tau$, the charge moved through the membrane, as a function of the applied potential. The solid line is the predicted behavior if the effective potential is 75% of the applied potential. The stippled line is the predicted behavior if the effective potential is equal to the applied potential. ▲ indicates charge moved during on-response, ○ indicates charge moved during off-response. The aqueous phases contained 0.1 M NaCl plus 7×10^{-8} M tetraphenylborate, 25°C.

FIGURE 6 Membrane polarization as a function of time. Log $(C(\infty) - C(t))$ is plotted vs. time. $C(\infty)$ denotes the amount of charge absorbed into one boundary phase of the membrane. $C(t)$ denotes the amount of charge transferred through the membrane at time t after applying the potential. The aqueous phase contained 0.1 M NaCl plus 7×10^{-8} M tetraphenylborate 25°C.

the Boltzmann distribution to calculate relative ion concentrations in the two boundary phases of the membrane at the end of a single current relaxation. If this is a valid approximation then the charge moved through the membrane as a function of potential should be described by Eq. 10. From Fig. 5 it can be seen that the agreement is excellent for $\beta = 0.75$, but poor for $\beta = 1.0$. β is obtained by calculating

$$\Delta N(V)/\tanh(\beta qV/2kT) = \text{“}N_{Abs}\text{”}$$

for all V, both on- and off-responses, and then calculating the mean value and standard deviation of the above quantity. β is varied systematically and the chosen value for β, and N_{Abs}, is that for which the standard deviation is least.

For the data given in Fig. 5 we find that the standard deviation was 3% of the mean value for $\beta = 0.75$, but 11% of the mean value for $\beta = 1.0$. Since β is less than 1 we conclude that the effective potential influencing the movement of tetraphenylborate ions is *not* equal to the applied potential but only to a certain fraction, β, thereof. For bacterial phosphatidylethanolamine membranes $\beta = 0.77 \pm 0.04$ (mean ±SEM), while $\beta = 0.92 \pm 0.04$ for dioleoylphosphatidylethanolamine membranes.

Membrane Conductance and Absorption of Ions as a Function of Concentration

In Fig. 7 the initial small signal (ohmic) conductance, $g(0,0)$, is plotted as a function of aqueous $TPhB^-$ concentration. The conductance is a linear function of $TPhB^-$ concentration below 3×10^{-7} M and goes through a maximum at 10^{-6} M. The presence of this maximum indicates some kind of interaction between ions absorbed into the boundary phases of the bilayer, possibly a limited number of absorption "sites"

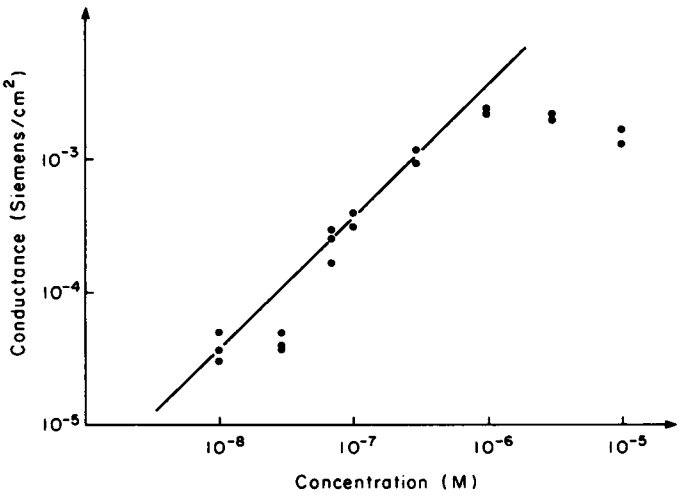

FIGURE 7 Membrane conductance $g(0,0)$, as a function of tetraphenylborate concentration. 0.1 M NaCl plus various concentrations of tetraphenylborate 25° ± 1.0°C.

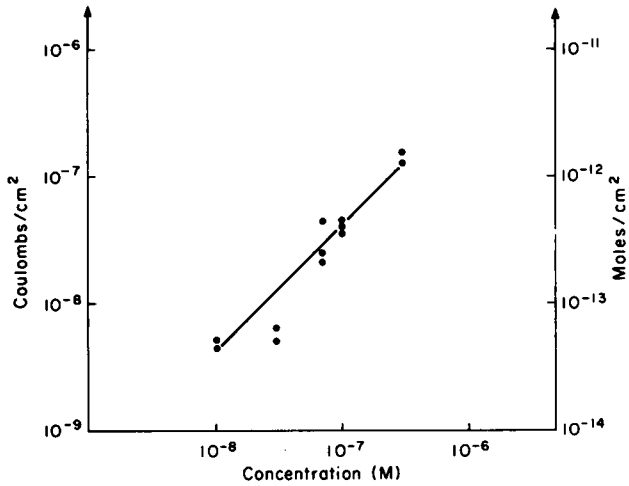

FIGURE 8 Absorption of tetraphenylborate ions into the membrane boundary phase. The amount of absorbed charge is obtained from the "best fit" charge transfer vs. applied potential curves as the value of N_{Abs} (and β) which gives the best fit of the observed data to Eq. 10, see text. 0.1 M NaCl plus various concentrations of tetraphenylborate, 25° ± 1.0°C.

(23). The nature of this interaction will not concern us here, since our experiments are done at $TPhB^-$ concentrations below 10^{-7} M, where these ion-ion interactions presumably can be neglected.

In Fig. 8, the total number of ions, actually coulombs, absorbed into one boundary region of a bilayer is plotted as a function of the concentration of $TPhB^-$. The number of ions absorbed is a linear function of $TPhB^-$ concentration up to 3×10^{-7} M $TPhB^-$. At higher concentrations of $TPhB^-$ ion movement across the membrane solution interface becomes significant compared with the ion movement through the center of the membrane. The time course of the current transient is no longer a single exponential, and diffusion polarization plays a significant role in determining the time course of the current. One can, therefore, not use Eq. 29 to calculate the number of ions absorbed into the membrane. From the data given in Fig. 8 one can calculate the distribution coefficient for $TPhB^-$ into the whole membrane to be approximately 10^4, assuming a uniform distribution within the entire membrane. The distribution coefficient of $TPhB^-$ ions into the membrane boundary regions is approximately 10^5. The depth of the potential energy minima is therefore about $12\,kT$, compared with the bulk aqueous phases.

Relaxation Time Constant as a Function of Applied Potential

In Fig. 9 the relaxation time constant, τ, is plotted as a function of the applied potential. For a membrane with a thickness of about 30 Å (footnote 6) and $\beta = 0.75$ one

[6]The specific membrane capacitance is 0.54 F/cm^2 ± 0.02, which increases during stirring to 0.62 ± 0.3 F/cm^2. The dielectric constant of the membrane interior is estimated to be 2.0 due to the low proportion of unsaturated fatty acid chains in the phospholipid (suppliers information).

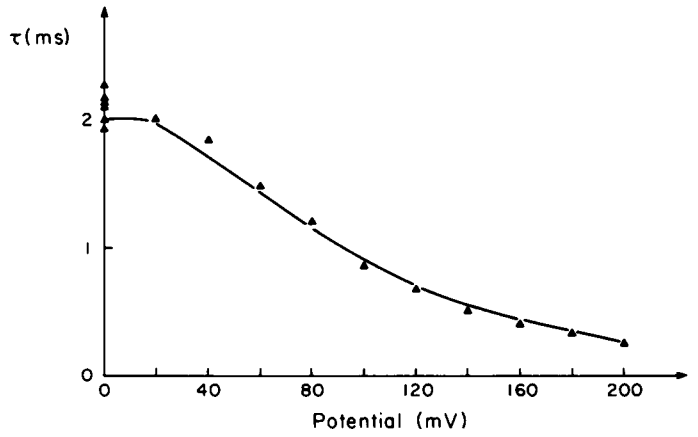

FIGURE 9 Relaxation time constant as a function of the applied potential. Time constants for the off-responses are plotted at $V = 0$. 0.1 M NaCl plus 7×10^{-8} M tetraphenylborate 25°C. Theoretical curve according to Eq. 30.

will from Eqs. 22, 24, 25, 28, and Table I predict that

$$\tau(V) = \tau(0) \cdot \exp[0.005(qV/kT)^2]/\cosh(0.75qV/2kT), \tag{30}$$

which is also plotted in Fig. 9.

A better test of Eq. 30 is to plot τ^{-1} vs.

$$\cosh(0.75qV/2kT) \cdot \exp[-0.005(qV/kT)^2],$$

in which case a straight line through the origin (0, 0) should result. This is, indeed, the case, as Fig. 10 shows. The correlation coefficient of the regression line is 0.999. The extrapolated time constant of the on-response to 0 mV, 2.1 ms, should be equal to the

TABLE I

COMPARISON OF $\omega(d)$ CALCULATED BY DIFFERENT METHODS, $\epsilon_m = 2.0$ IN ALL CASES

Membrane thickness, d	Neumcke and Läuger (38)	Haydon and Hladky (18)	Present article
Å			
25	0.0045	0.0027	0.0043
30	0.0052	0.0032	0.0050
35	0.0059	0.0038	0.0056
40	0.0065	0.0043	0.0062
45	0.0071	0.0049	0.0069
50	0.0077	0.0054	0.0074
55	0.0082	0.0059	0.0079
60	0.0087	0.0065	0.0084

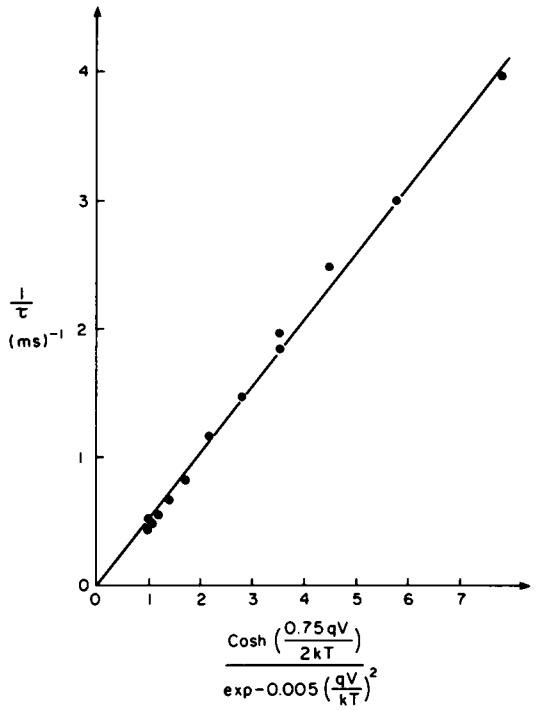

FIGURE 10 Voltage dependence of the relaxation time constant. The experimental values of τ^{-1} are plotted as a function of $\exp[-0.005(qV/kT)^2]/\cosh(0.75qV/2kT)$. A straight line through (0,0) should result. 7×10^{-8} tetraphenylborate in 0.1 M NaCl, 25°C.

time constant for the off-response, 2.13 ± 0.04 ms (mean ± SEM). τ for the off-response is independent of the applied potential during the on-response, as it should be according to Eq. 28. τ is independent of the concentration of $TPhB^-$ up to a concentration of 3×10^{-7} M. At higher concentrations we find that the apparent time constant increases with increasing $TPhB^-$ concentration due to diffusion polarization.

Membrane Conductance as a Function of Applied Potential

From Eqs. 17, 18, 24, 25, and Table I one can derive a theoretical expression for the voltage dependence of the initial conductance $g(V,0)/g(0,0)$ to be

$$g(V,0)/g(0,0) = (2kT/0.75qV)\cdot(\sinh[0.75qV/2kT]/\exp[0.005(qV/kT)^2]), \quad (31)$$

where we again assume $d = 30$ Å and $\beta = 0.75$. We have dropped subscripts since the conductance has been normalized.

In Fig. 11 we have plotted the experimental values for $g(V,0)/g(0,0)$ as well as the prediction of Eq. 31. For comparison we have also plotted the functions

$$g(V,0)/g(0,0) = (2kT/qV)\cdot\sinh(qV/2kT), \quad (32)$$

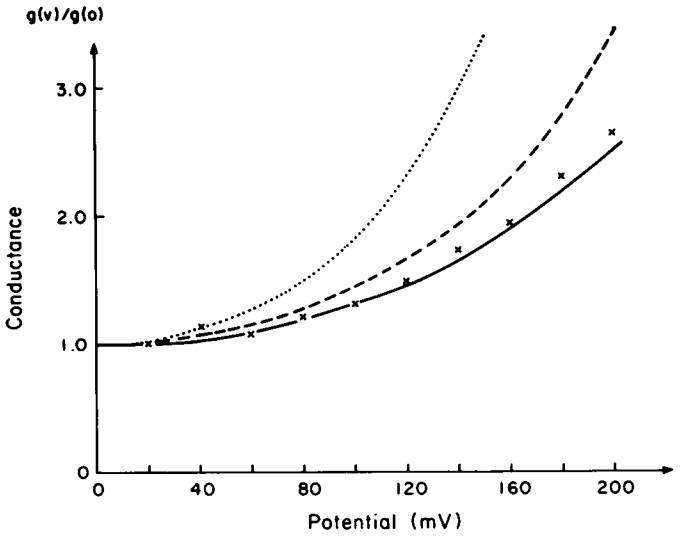

FIGURE 11 Initial conductance, $g(V,0)$, as a function of the applied potential. 7×10^{-8} M tetraphenylborate plus 0.1 M NaCl, 25°C. ———, theoretical curve according to Eq. 31; - - - - - - - - - - - -, theoretical curve according to Eq. 32; . . . . . , theoretical curve according to Eq. 33.

and

$$g(V,0)g(0,0) = (2kT/0.75qV)\cdot\sinh(0.75qV/2kT), \tag{33}$$

which give the predicted voltage dependence of $g(V,0)/g(0,0)$, as obtained by Ketterer et al. (23), assuming that the total or only 75% of the applied potential is effective, respectively. It is apparent that Eq. 33 does not predict the experimental data at all while Eqs. 31 and 32 both provide a reasonably good agreement between theory and experiment. The agreement, however, is significantly better with Eq. 31. The experimentally observed relationship of $g(V,0)/g(0,0)$ vs. V is thus consistent with a model for ion transport within lipid bilayers where the potential energy barrier for ion transport is assumed to be the image-force barrier.

Membrane Conductance as a Function of Time

From Eq. 15 A it is predicted that the membrane conductance will change with time during the current-transients. We can obtain this information, indirectly, by studying the initial membrane conductance during the off-response, $g_{V,t}(0,0)$. If the on-response lasts for more than 10τ then $E(t) = \beta V$. From Eqs. 10 and 27 we obtain, assuming $\beta = 0.75$, that

$$g_{V,t}(0,0)/g(0,0) = (2kT/q)[\tanh(0.75qV/2kT)/0.75V], \tag{34}$$

where $g(0,0)$ denotes the small-signal conductance for the off-response conductance which is equal to the small-signal conductance for the on-response. In Fig. 12, we

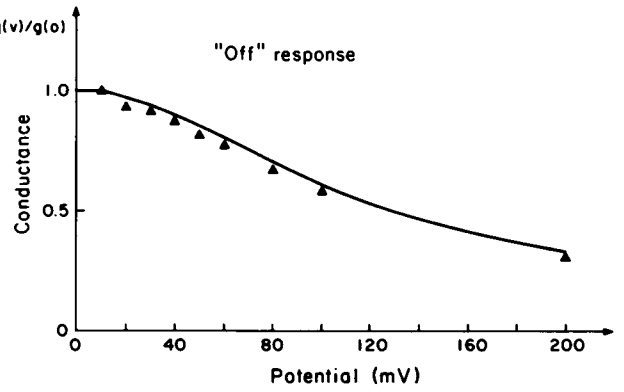

FIGURE 12 Initial conductance for the "off" response as a function of the "on" potential. The solid line is calculated according to Eq. 31. 0.1 M NaCl plus 7×10^{-8} M tetraphenylborate 25°C.

plotted Eq. 34 as well as experimentally obtained values for $g_{V,t}(0,0)/g(0,0)$. The small deviations may be due to an overestimate of $g(0,0)$. Fig. 12 does not provide information about $W(x)$, but it confirms our determination of β.

DISCUSSION

The transport of lipid soluble ions through lipid bilayers can serve as a model for carrier-mediated ion transport through the interior of these membranes. The analysis of these transport mechanisms has generally been based on the potential dependence of membrane conductance (4, 7, 17, 20, 21, 23, 27–29, 38, 46, 47), or relaxation time constant (4, 23, 27, 29, 47). In this article we show that lipid soluble ions possess the advantage that one can *measure* the number of ions absorbed into one boundary phase of a lipid bilayer, independent of any specific kinetic model for the transport mechanism. This is a fairly unique property of $TPhB^-$, dipicrylamine (23), and possibly a few other species, and it makes $TPhB^-$ a very useful tool with which to study the properties of lipid bilayers. Thus we can show that only a certain fraction, β, of the applied potential is effective in moving $TPhB^-$ ions, and possibly many other ions, through lipid bilayers. This determination of β acts as a model-independent constraint any satisfactory kinetic model for ion transport through lipid bilayers must satisfy.

Several objections may be raised at this point. Firstly, the membrane properties may change with the applied potential, which will affect both the charge measurements and the initial conductance measurements. It is well known that membrane area increases and membrane thickness decreases with applied potential (3, 52). Measurements of membrane capacitance in the absence of $TPhB^-$ indicate that below 200 mV these area and thickness changes contribute less than 3% to the "slow" current transient (the first 10 ms) in the presence of $TPhB^-$, unless major changes not seen in the capacitance measurements occur in membrane structure. Secondly, there may be lateral diffusion of $TPhB^-$ into the bilayer from the surrounding torus. This will tend to overestimate

the amount of $TPhB^-$ that is absorbed into the bilayer proper. The error involved is, however, small due to the low diffusion coefficient which may be estimated to be 4×10^{-8} cm^2/s (see later).

Thirdly, we use the Boltzmann distribution to calculate the relative ion concentrations in the two boundary phases at the end of the current relaxation. The Boltzmann distribution is an equilibrium distribution, and can, therefore, only be approximately valid since there is net ion transport occurring both across the membrane-solution interfaces and through the membrane interior. This measured current is the sum of a diffusion current, I_D, and a drift current, I_V, where

$$I_D = -qukT(dC/dx),$$

and

$$I_V = qC[q(d\phi/dx) - (dW/dx)],$$

and I_D and I_V are in opposite directions. The net current is very small compared with each of the two component currents (compare $I(0)$ for the off response with $I(4\tau)$ for the on-response in Figs. 2 and 3). This situation is similar to the *p-n* junction in semiconductors (ref. 50, pp. 304–306). In this case it is concluded that the Boltzmann distribution is a valid approximation in the presence of small, but finite, net currents. The Boltzmann distribution should therefore also be a reasonable approximation in our case. Consequently we may regard β as determined here to be a valid estimate of the actual fraction of the applied potential that is effective in influencing ion movement within the bilayer.

β does not give any unambiguous determination of the location of the potential energy minima within the membrane. Firstly, because such a determination would require information about the electrical potential profile within the membrane, which in practice would be the constant field approximation, and this approximation is certainly wrong near the boundary regions due to the quite high space charge. Secondly, such a determination would be dependent on a macroscopic model (uniform slab of hydrocarbon with plane boundaries, no potential drop over the polar head groups) of the microscopic reality. It is, however, of interest to note that one can calculate an effective potential of 72% assuming that the center of the $TPhB^-$ ions are located 4.2 Å (radius of $TPhB^-$ [14]) into a membrane with a thickness of 30 Å. Furthermore, β increases with increasing membrane thickness: in bacterial phosphatidylethanolamine membranes, $d = 30$ Å, $\beta = 0.77 \pm 0.04$, while $\beta = 0.92 \pm 0.04$ in dioleoylphosphatidylethanolamine membranes, $d = 46$ Å.[7]

Another objection is that we use instantaneous conductances to obtain information about the potential energy barrier(s) to ion transport within the bilayer. This problem is, however, more apparent than real, because we can get the same information from the potential dependence of the relaxation time constant as from the poten-

[7]Calculated from capacitance data (21), assuming the dielectric constant of the membrane interior to be 2.1.

tial dependence of conductance (compare Eqs. 17 and 22). Furthermore, one may calculate the characteristic time constant for the instantaneous relaxation of ionic profiles within the bilayers to be 1–3 μs (see Appendix I), while the time constant of the current transient varies from 0.2 to 2 ms. We may, therefore, consider the system to be in a pseudostationary state where the Nernst-Planck electrodiffusion equations are applicable (39).

A similar conclusion can be reached from the observation that the time constant of the off-response is independent of the applied potential during the on-response, but dependent on the off-potential which was usually 0 mV. In a few experiments we applied a steady potential difference across the membrane, 60 and 120 mV. We found, as expected, that the off-response time constant indeed was only dependent on the off-potential.

The general behavior of the present system is therefore phenomenologically similar to the "gating currents" in the squid giant axon (2, 24), with respect to the time course of the currents and their potential dependence. We therefore believe that gating currents can be analyzed by a model very similar to the present.

The kinetics of $TPhB^-$ current relaxations within lipid bilayers have previously been studied by Ketterer et al. (23) who observed a behavior similar to the one described here. The main difference between their approach and the present is that Ketterer et al. used an Eyring rate theory model to describe all their data. So they *assume* $\beta = 1$ and derive the value of N_{Abs} from a model-dependent analysis of the current transients. These authors found that the behavior of $TPhB^-$ in dioleoyllecithin membranes was adequately described by the rate theory model up to $V = 125$ mV, presumably due to

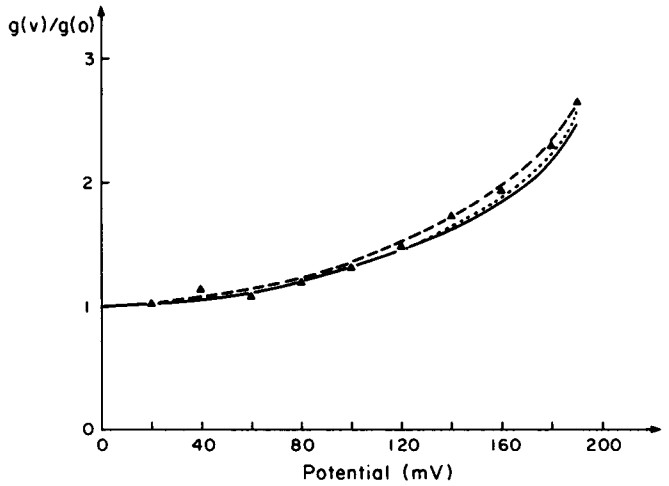

FIGURE 13 Theoretically predicted conductance-voltage characteristics. ———, image-force potential energy barrier $\beta = 0.75$, calculated according to Eq. 31; – – – –, Eyring rate theory model, $\beta = 0.65$, calculated according to Eq. 37; . . . . . , trapezoidal energy barrier with flat top from $x = 0.2d$ to $x = 0.8d$, $\beta = 0.95$, calculated according to Eq. 38. Experimental points from Fig. 11.

the greater thickness of these membranes compared with ours. It should, however, be noted that they could not describe the behavior of the dipicrylamine anion using their model.

The general expression for initial membrane conductance (actually barrier conductance) is

$$g(V,0) = \frac{Auq^2Cz^2 \cdot \sinh(z\beta qV/2kT)}{(z\beta qV/2kT) \cdot \exp(-zqV/2kT) \int_{\eta}^{d-\eta} \exp([W_1(x) + zq\phi(x)]/kT)\,dx}. \quad (35)$$

The numerator of Eq. 35 is a well-known function of V, apart from a determination of β, and does therefore not contain much information about the transport mechanism. The success of any model for ion transport through lipid bilayers will, therefore, be dependent on the properties of the integral

$$\int_{\eta}^{d-\eta} \exp([W_1(x) + zq\phi(x)]/kT)\,dx. \quad (36)^8$$

One can either evaluate the above integral in terms of a specific model for $W_1(x)$ (21, 23, 29, 38), or one can use the value of the integral, as deduced from current-voltage characteristics, to obtain information about $W_1(x)$ (17). In both cases it is of crucial importance to determine the correct value for β. For any arbitrary value of $\beta < 1$, it is possible to find a function $B(x)$ to represent the shape of the potential energy barrier, such that the experimentally observed current-voltage curves are correctly predicted. This is illustrated in Fig. 13, where the experimental data from Fig. 11 are plotted together with Eq. 31 and the functions

$$g(V,0)/g(0,0) = (2kT/0.65qV) \cdot \sinh(0.65qV/2kT), \quad (37)$$

and

$$g(V,0)/g(0,0) = [0.6 \cdot \sinh(0.95qV/2kT)]/[0.95 \cdot \sinh(0.6qV/2kT)]. \quad (38)$$

Eq. 31 is the prediction when the shape of $W_1(x)$ in the center of the membrane is

[8] An implicit assumption in writing Eq. 35, and of our analysis, is that the movement of $TPhB^-$ ions within the bilayer is smooth. This may not be a good assumption for the movement of an ion with a radius of 4 Å through a membrane 30 Å thick. Ion movements may occur through small "jumps" between local potential energy minima (21, 29) in which case the integral Eq. 36 should be replaced by the appropriate finite sum. One can, however, calculate that the potential dependence of this finite sum is identical to that of the integral for jump lengths up to 4 Å in a 30 Å thick membrane (for potentials up to 200 mV). We therefore conclude that the Nernst-Plank equations do provide a reasonable basis to both stationary and pseudostationary transport in lipid bilayers.

given by the shape of the image-force barrier as calculated in Appendix III and β = 0.75.

Eq. 37 is the predicted value for $g(V,0)/g(0,0)$ when $W(x)$ is equal to $\delta[x - (d/2)]$ the Dirac delta function and β = 0.65. This expression is identical to the predictions from the Eyring rate theory. Eq. 38 is the prediction when $W(x)$ is trapezoidal with a high horizontal plateau in the membrane from $x = 0.2\,d$ to $x = 0.8\,d$, and β = 0.95.

The agreement between theory and experiment is excellent in all three cases, even though the interpretation is quite different. It is, however, clear that once we have determined β we have also ruled out both Eq. 37 and Eq. 38, but we still obtain agreement with Eq. 31. We, therefore, conclude that the potential energy barrier to ion transport within lipid bilayers is closely related to the image-force potential energy barrier. It should be stressed that this does not and cannot *prove* that the potential energy barrier is the image-force barrier. One can, for example, with β = 0.75, also describe the experimental data reasonably well with a trapezoidal barrier that is horizontal from $x = 0.35\,d$ to $x = 0.65\,d$ (see also ref. 21, p. 79). This latter shape of the energy barrier does not, however, have any obvious physical interpretations.

If our model is correct then we should be able to predict the membrane conductance from the mobility, u_m, of $TPhB^-$ within the membrane, the distribution coefficient of the "neutral" TPhB into the membrane, K_s, the dipole potential at the membrane solution interface V_D and $\int_{\eta}^{d-\eta} \exp(W_e(x)/kT)\,dx$. The conductance is then approximated by

$$g(0,0) \approx [u_m q^2 A C_{Aq} K_s \cdot \exp(-zqV_D/kT)]/\int_{\eta}^{d-\eta} \exp(W_e(x)/kT)\,dx \quad (39)$$

The mobility of $TPhB^-$ in the membrane may be estimated from its mobility in water, u_{H_2O}, 1.25×10^{11} m · s^{-1} · N^{-1} (44) and the relative viscosity of water, η_{H_2O}, 0.9 cP (51), to that of the hydrocarbon interior, η_m, ~ 1 P (9, 42), using the Walden product (6) $u_m \cdot \eta_m = u_{H_2O} \cdot \eta_{H_2O}$. We obtain $u_m \sim 1 \times 10^9$ m · s^{-1} · N^{-1}. The distribution coefficient of the uncharged TPhB between membrane and water is not known, but may be estimated from the solubility of tetraphenylmethane in water 1.6×10^{-8} M (10) and the solubility of tetraphenylmethane in benzene, 1.5×10^{-2} M (36). A reasonable distribution coefficient between water and membrane is therefore 10^6. The dipole potential at the membrane-solution interface can be estimated from the relative conductances of $TPhB^-$ and its positive counterpart tetraphenylarsonium ($TPhAs^+$) in lipid bilayers. In bacterial phosphatidylethanolamine we obtain a conductance of 1×10^{-8} S/cm^2 for 10^{-5} M $TPhAs^+$ in the aqueous phases[9] (O. S. Andersen and M. Fuchs, manuscript in preparation), compared to an estimated conductance at 3.5×10^{-2} S/cm^2 with $TPhB^-$ in the same concentration. The relative conductance is, therefore, 3×10^6 (compare also Le Blanc [31]) and the estimated dipole potential is 190 mV

[9]Membrane conductance does not increase linearly with $TpHAs^+$ concentration over a wide concentration range. However, at low concentrations of $TPhAs^+$ (and very low membrane conductances) there appears to be a region with a linear relation between $TPhAs^+$ concentration and membrane conductance.

positive inside the membrane. This calculation assumes that the free energies of hydration for $TPhB^-$ and $TPhAs^+$ are identical. Single ion solvation energies cannot be measured but may be calculated using some extrathermodynamic assumptions (6, 10, 14, 26), one of which is that the solvation energies of $TPhB^-$ and $TPhAs^+$ are identical (10, 14, 26). Recently, however, it has become clear that this is not the case (8, 22, 26). It has been suggested (8) that one should use the Buckingham theory of ion-quadropole interactions (see, for example, ref. 6) to estimate the difference between the solvation energies of $TPhAs^+$ and $TPhB^-$. The difference becomes about 25 KJ/mol, using a radius for both ions of 4.2 Å, which means that $TPhAs^+$ should have a conductance about 10,000 times higher than $TPhB^-$ in the absence of any dipole potential. The estimated dipole potential is therefore +310 mV.[10] This value is considerably less than the surface potential of phosphatidylethanolamine at the air-water interface, 480–520 mV (21). The physical meaning of these two potentials is, however, quite different so that a quantitative comparison is not appropriate.

The integral was evaluated using the image-force calculation in the Appendix, using $r = 4.2$ Å, $d = 30$ Å, $\epsilon_m = 2$. The estimated conductance comes out to be 2×10^{-4} S/cm^2 at 10^{-7} M $TPhB^-$ in reasonable agreement with the measured value of 3.5×10^{-4}. The agreement does not show whether the chosen potential energy is correct or not, but it does indicate that the basically macroscopic theory we have developed is adequate to describe the movement of charged particles with a radius of 4 Å through membranes 30–40 Å thick.

Another test of the general model is whether $\tau(0)$ has any meaningful relation to the diffusional transit time, τ_T, for a single particle through the membrane.

$$\tau_T \sim (d^2/2D_m) \sim 1\ \mu s,$$

while $\tau(0)$ is 2.0 ms. The ratio $\tau(0) \cdot \tau_T^{-1}$ should be approximately equal to the ratio

$$\frac{\int_{\eta}^{d-\eta} \exp[W_1(x)/kT]\,dx}{d} = \frac{\int_{\eta}^{d-\eta} \exp[W_e(x)/kT]\,dx}{d \cdot \exp[W_e(\eta)/kT]}.$$

Using $d = 30$ Å, $r = 4.2$ Å, $\epsilon_m = 2$, we obtain that $\exp[W_e(\eta)/kT] = 3 \times 10^7$ or $W_e(\eta) \sim 17\,kT$ (relative to a $W_e(d/2) = 26\,kT$). $W_e(x)$ has the value of $17\,kT$ at $x = 4.5$ Å. It is gratifying that this calculation is consistent with our finding that $\beta < 1$. This estimate indicates that $TPhB^-$ ions are absorbed into the bilayer interior *inside* the dipole region, a result that would be expected a priori.

The potential energy barrier within bacterial phosphatidylethanolamine bilayers has also been studied by Hall et al. (17) and by Hladky (21). Both used the potassium complex of nonactin (K^+-nonactin) as the current carrier and they obtained experimental

[10]This potential difference is the so-called Galvani or inner potential difference. It is *in principle* not measurable (6, 15, 16, 40), but it may be estimated using the same extrathermodynamic assumptions as are used to estimate "single ion" free energies of solvation (see also Guggenheim [16]).

results that were qualitatively similar to ours. In both cases the current increased less steeply with potential than the sinh ($qV/2kT$) relation predicted. Similar results have also been reported by Laprade et al. (27) for glycerol dioleate/decane membranes and by Hladky (21) on glycerolmonooleate-hexadecane membranes. Both Hall et al. (17) and Hladky (21) concluded that the potential energy barrier in bacterial phosphatidylethanolamine membranes is trapezoidal with a flat top in the middle of the membrane, in apparent conflict with our conclusions. It is possible that the potential energy barrier in the middle of the membrane observed for K^+-nonactin is quite different in shape from that observed for $TPhB^-$, due to the difference in size and charge of the two species. This is a rather unlikely possibility since the radius of the K^+-nonactin complex is only 6.3 Å (43)[11] compared with 4.2 Å for $TPhB^-$. Once the ion-ion carrier complex is formed there is, therefore, little reason to expect that it will behave radically different from the $TPhB^-$ ion. The main factor that determines the shape of the potential energy barrier in the middle of the membrane is the electrostatic interaction between ion and the aqueous phases which should not be overly dependent on sign, and size of an ion in the interior of the membrane. We, therefore, conclude that the shape of the potential energy barrier should be similar for the two current carrying species. *If* the potential energy barrier in the middle of the membrane is the same for both K^+-nonactin and $TPhB^-$, then the behavior of K^+-nonactin near the interfaces must differ from what is assumed by both Hall et al. and Hladky. One suggestion is that there exists a significant potential energy barrier for ion movement across the membrane-solution interfaces and a potential energy minimum for the ion-ion carrier complex within the membrane. The rate constants for association and dissociation of the K^+-nonactin complex will therefore be voltage dependent, and the existence of the barrier at the membrane-solution interfaces can contribute significantly to the observed current-voltage characteristics. Both the current-voltage data of Hall et al. and Hladky, as well as the rectification studies of Hall et al. would be consistent with such a mechanism. In fact, Hladky found that to explain his very accurate data obtained on glycerolmonooleate-hexadecane membrane, it was necessary to assume that the reaction rate constants changed with the applied potential. This does not "prove" that the potential energy barrier observed by K^+-nonactin in the middle of the membrane is the image-force barrier, but it is remarkable that Hladky (21) found that an image-force barrier, with $\omega = 0.005$ was consistent with his data. For a glycerolmonooleate-hexadecane membrane with a thickness of 32 Å, the predicted ω from our image-force calculations is 0.0052.

We conclude that tetraphenylborate is very suitable to study details of ion transport within lipid bilayers. The transport may be described by the generalized Nernst-Planck equations provided one uses the image-force barrier to represent the potential energy barrier to ion transport in the middle of the membrane. An essential step in such an analysis is the determination of β or the effective potential.

We suggest that such a formalism also can describe the movement of K^+-nonactin

[11] The Stokes radius of the K^+-nonactin complex in acetonitrile is even lower, 4 Å (41).

through the membrane interior, and that comparison of current-voltage characteristics for $TPhB^-$ and ion-ion carrier complexes may provide information about behavior of the carrier near the interfaces.

APPENDIX I

Calculation of the Charging Time Constant within a Lipid Bilayer

A nonlinear current-voltage characteristic of a membrane implies that the concentration profile(s) within the bilayer is (are) a function of the applied potential (13). An applied potential will therefore cause a redistribution of ions within the membrane. This redistribution of ions is not instantaneous, but occurs with a characteristic time constant τ_C (39). These concentration changes will give rise to changes in the electric field within the membrane since, for $z = -1$,

$$\partial^2\phi/\partial x^2 = +qC(t)/(\epsilon \cdot \epsilon_0), \tag{40}$$

where ϵ_0 is the capacitivity of vacuum, and ϵ is the relative dielectric constant of the medium. This change in the electrical field will furthermore give rise to a "displacement" current, I_C,

$$I = +\epsilon \cdot \epsilon_0 \cdot (\partial^2\phi/\partial x \partial t). \tag{41}$$

Note the sign convention. We can, therefore, conclude that the field within the membrane cannot be strictly constant during the charge redistribution period, and that the measured current I, is the sum of an ionic current I_I and I_C,

$$I = I_I + I_C. \tag{42}$$

The first of these problems is minor, since the field will be essentially constant, even during the charging period, provided that the ion concentration within the membrane is sufficient to ensure that $C(t) \ll 5 \times 10^{-5}$ M (29) for all t[5]. To obtain a solution to the second problem we have

$$\begin{aligned} I(t) &= I_I(x,t) + I_C(x,t) \\ &= -uq[kT(\partial C/\partial x) - Cq(\partial\phi/\partial x) + C(\partial W/\partial x)] + [(\epsilon \cdot \epsilon_0 \cdot \partial^2\phi)/\partial x \partial t], \end{aligned} \tag{43}$$

which may be integrated with respect to t, substituting $E(x,t) = -(\partial\phi/\partial x)$, and we obtain

$$\begin{aligned} E(x,t) - E(x,0) \cdot \exp[-q^2Cut/(\epsilon \cdot \epsilon_0)] = [1/(\epsilon \cdot \epsilon_0)] \int_0^t \{I + [qukT(\partial C/\partial x)] + \\ [Cqu(\partial W/\partial x)]\} \exp[q^2Cu(t - \zeta)/(\epsilon \cdot \epsilon_0)]\, d\zeta. \end{aligned} \tag{44}$$

To study the time course of the charging current further one may write

$$(\epsilon \cdot \epsilon_0)/q^2Cu = L_D^2/D_m = \tau_C, \tag{45}$$

where L_D is the Debye-length (6), and D_m is the diffusion coefficient for $TPhB^-$ within the membrane and L_D^2/D_m is approximately the time necessary to establish diffusion equilibrium

in a region of thickness L_D. We assume that $L_D \gg d$ (the assumption that the steady-state field is constant) so Eq. 44 is not appropriate for a membrane with a thickness much less than L_D. A reasonable approximation for τ_C will be

$$\tau_C = d^2/D_m. \tag{46}$$

If $d = 30$ Å and $D = 4 \times 10^{-8}$ cm^2/s (see the Discussion section) we have $\tau_C = 2.0$ μs. If the time constant of the observed current is much longer than τ_C, a useful approximation to the integral in Eq. 44 is

$$(+1/q^2Cu) \cdot \{I(t) + [qukT(\mathrm{d}C/\mathrm{d}x)] + [Cqu(\mathrm{d}W/\mathrm{d}x)]\}, \tag{47}$$

and we obtain for $t \gg \tau_C$ that

$$I(t) = -qu\{kT(\mathrm{d}C/\mathrm{d}x) - [qC(\mathrm{d}\phi/\mathrm{d}x)] + [C(\mathrm{d}W/\mathrm{d}x)]\}. \tag{48}$$

APPENDIX II

Identity of Eqs. 15 A and 15 B for a Pseudostationary Nernst-Planck Electrodiffusion Regime

We have

$$j(t) = -Au\{kT(\mathrm{d}C/\mathrm{d}x) + C(x,t)[(\mathrm{d}W_1/\mathrm{d}x) - q(\mathrm{d}\phi/\mathrm{d}x)]\}, \tag{49}$$

where we assume u to be independent of x. We have furthermore substituted $W_1(x)$ for $W(x)$, so that $W_1(\eta) = W_1(d - \eta) = 0$. We integrate Eq. 49 to determine the concentration profile through the membrane and obtain, setting $C(\eta,t) = C_I(t)$ and $C(d - \eta,t) = C_{II}(t)$, that

$$C(x,t) = \exp[-(W_1(x) - q\phi(x))/kT] \cdot \{C_I(t) \cdot \exp(-q\phi(\eta)/kT) + [C_{II}(t) \cdot \exp(-q\phi(d - \eta)/kT) - C_I(t) \cdot \exp(-q\phi(\eta)/kT)] \cdot \Phi(x)\}. \tag{50}$$

Where we have substituted

$$\int_\eta^x \exp[W_1(y) - q\phi(y)/kT]\,\mathrm{d}y \Big/ \int_\eta^{d-\eta} \exp[W_1(y) - q\phi(y)/kT]\,\mathrm{d}y = \Phi(x), \tag{51}$$

where y is an integration variable into Eq. 50. Eq. 50 is substituted into Eq. 15 B to obtain

$$g(V,t) = \frac{A}{\displaystyle\int_\eta^{d-\eta} \frac{\exp([W_1(x) - q\phi(x)]/kT)\,\mathrm{d}x}{uq^2 \cdot \{C_I(t) \cdot \exp(-q\phi(\eta)/kT) + [C_{II}(t) \cdot \exp(-q[\phi(d - \eta)]/kT) - C_I(t) \cdot \exp(-q\phi(\eta)/kT)] \cdot \Phi(x)\}}} \tag{52}$$

We change the variable of integration to be $z = \Phi(x)$

$$z(\eta) = 0; z(d - \eta) = 1,$$

and we obtain

$$g(V,t) = \frac{Auq^2}{\int_{\eta}^{d-\eta} \exp([W_1(x) - q\phi(x)]/kT)\,dx} \times$$

$$\frac{1}{\int_0^1 dz/\{[C_I(t)\cdot\exp(-q\phi(\eta)/kT)] + [C_{II}(t)\cdot\exp(-q\phi(d-\eta)/kT)] - [C_I(t)\cdot\exp(-q\phi(\eta)/kT)z]\}}, \quad (53)$$

or

$$g(V,t) = \frac{Auq^2}{\int_{\eta}^{d-\eta} \exp([W_1(x) - q\phi(x)]/kT)\,dx} \times \frac{C_{II}(t)\cdot\exp[-q\phi(d-\eta)/kT] - C_I(t)\cdot\exp[-q\phi(\eta)/kT]}{\ln[C_{II}(t)/C_I(t)] - [(q\phi(d-\eta) - q\phi(\eta))/kT]}, \quad (54)$$

so that we finally obtain that

$$g(V,t) = \frac{-AukTq[C_{II}(t)\cdot\exp(-\beta qV/2kT) - C_I(t)\cdot\exp(\beta qV/2kT)]}{[\beta V - (kT/q)\cdot\ln(C_{II}/C_I)]\cdot\exp(qV/2kT)\int_{\eta}^{d-\eta}\exp([W_1(x) - q\phi(x)]/kT)\,dx}, \quad (55)$$

which is identical to Eq. 15 A.

APPENDIX III

Calculation of the Image-Force Potential Energy Barrier

An ion of radius r within a lipid membrane of low dielectric constant, ϵ_m, will be attracted towards the surrounding aqueous phases which have a high dielectric constant, ϵ_{H_2O} (18, 21, 29, 38). This attraction is due to the polarization charges which are induced at the membrane-solution interfaces by the ion. Under certain circumstances one can calculate this attractive force, starting with a calculation of the attractive force between the ion and a single plane interface. Firstly, if the aqueous phase is a perfect dielectric and the ion ideally nonpolarizable we obtain (5)

$$F_1(x) = -[(\epsilon_{H_2O} - \epsilon_m)/(\epsilon_{H_2O} + \epsilon_m)]\cdot[q^2/4\pi\epsilon_0\epsilon_m(2x)^2].$$

Secondly, if the aqueous phase is a perfect conductor and the ion ideally nonpolarizable we obtain (5)

$$F_2(x) = -[q^2/4\pi \cdot \epsilon_0 \cdot \epsilon_m (2x)^2].$$

Thirdly, if the aqueous phase is a perfect conductor and the ion a conducting sphere of radius r, we have (45)

$$F_3(x) = + \frac{q^2 \cdot \sum_{n=1}^{\infty} \operatorname{csch}(n\alpha)[\coth(\alpha) - n \cdot \coth(n\alpha)]}{8r^2\pi\epsilon_0\epsilon_m \cdot \left\{\sinh(\alpha) \cdot \sum_{n=1}^{\infty} \operatorname{csch} n\alpha\right\}^2},$$

where $\alpha = \operatorname{arccosh}(x/r)$, and x is the distance from the interface, $x > r$. F_1 may be regarded as a lower limit on the force, because the $TPhB^-$ ions are polarizable and the presence of electrolytes in the aqueous phases are neglected. Similarly, F_3 is an upper bound on the force, because the $TPhB^-$ ions are not perfectly conducting spheres and the aqueous phases are relatively poor conductors. We, therefore, choose F_2 to represent the attractive force between the ion and the aqueous phases. Following a procedure otherwise similar to that of Neumcke and Läuger (38) we obtain that the total force, $F(x)$, on the ion within the membrane is

$$F(x) = \frac{-q^2}{16\pi\epsilon_0\epsilon_m} \cdot \left\{\frac{1}{x^2} + \frac{1}{d^2} \cdot \sum_{n=1}^{\infty} \left(\frac{1}{[n + (x/d)]^2} - \frac{1}{[n - (x/d)]^2}\right)\right\}, \qquad (56)$$

where d is membrane thickness. In the interior of the membrane ($r < x < d - r$), the potential energy $W_e(x)$ is

$$W_e(x) = W_e(r) - \int_{r+}^{x} F(x)\,dx$$

$$= W_e(r) + \frac{q^2}{16\pi\epsilon_0\epsilon_m d} \times$$

$$\left\{\frac{d}{r} - \frac{d}{x} + \frac{x - r}{d} \cdot \sum_{n=1}^{\infty} \left(\frac{1}{[n + (x/d)]\,[n + (r/d)} - \frac{1}{[n - (x/d)]\,[n - (r/d)]}\right)\right\} \qquad (57)$$

$$= W_e(r) + \frac{q^2}{16\pi\epsilon_0\epsilon_m d} \cdot [\psi(x/d) - \psi(r/d) + \psi(1 - x/d) - \psi(1 - r/d)], \qquad (58)$$

where ψ is the digamma function (1).

To calculate $W_e(x)$, it is necessary to evaluate $W_e(r)$, a procedure that is largely arbitrary because the electrical potential difference between two dissimilar phases is experimentally inaccessible (15, 40), and of uncertain physical significance in the present context (see also foot-

note 9). A useful expression is

$$W_e(r) = \frac{q^2}{8\pi\epsilon_0 r}\left(\frac{1}{\epsilon_m} - \frac{1}{\epsilon_{H_2O}}\right) - \frac{q^2}{16\pi\epsilon_m e_0 r}, \tag{59}$$

modified from Neumcke and Läuger (38). An expression similar to Eq. 58 was obtained by Haydon and Hladky (18). These authors did, however, evaluate $W_e(r)$ to be

$$\frac{q^2}{8\pi\epsilon_0}\cdot\left\{\frac{1}{r}\left(\frac{1}{\epsilon_m} - \frac{1}{\epsilon_{H_2O}}\right) - \frac{1}{2\epsilon_m d}\times \left[\frac{d}{r} + \frac{d}{d-r} + 2\psi(1) - \psi\left(1 + \frac{r}{d}\right) - \psi\left(2 - \frac{r}{d}\right)\right]\right\}. \tag{60}$$

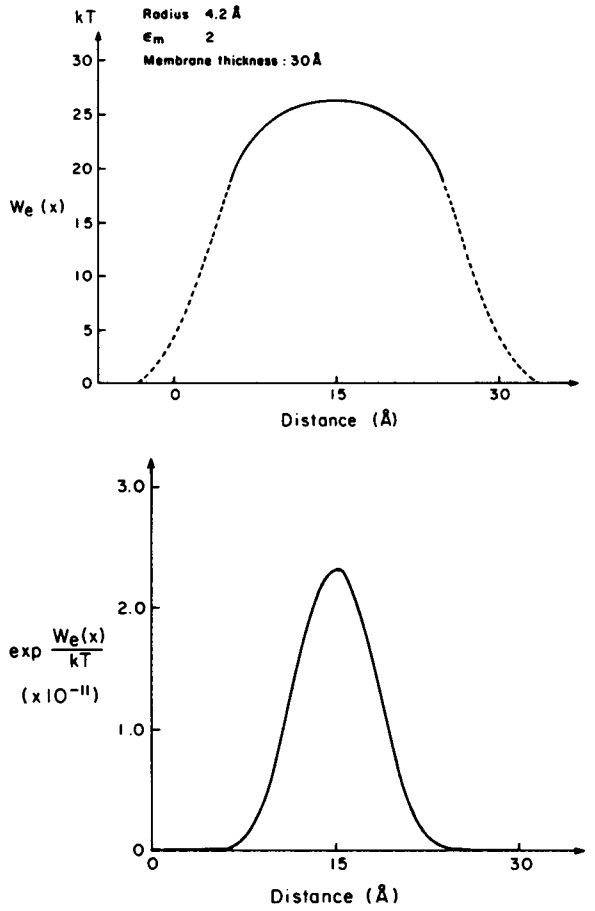

FIGURE 14 *Top (A)*: Image-force potential energy barrier, for an ion of radius 4.2 Å, in a membrane of thickness 30 Å and dielectric constant 2.0. Energy is expressed in units of kT and calculated after Eqs. 57 and 59. *Bottom (B)*: Plot of $\exp[W_e(x)/kT]$ vs. x. Parameters are as for Fig. 14A.

$W_e(x)$ was calculated numerically for $r < x < d - r$ using Eq. 57, see Fig. 14 A. A third degree polynomial was used to calculate $W_e(x)$ in $-r < x < r$ and $d - r < x < d + r$. The important function is, however, not $W_e(x)$ but $\exp(W_e(x)/kT)$ which is plotted in Fig. 14 B. It is apparent that even though $W_e(x)$ is fairly flat in the middle of the membrane, $\exp(W_e(x)/kT)$ has a distinct peak in the middle. The only significant contribution to

$$\int_{-r}^{d+r} \exp([W_e(x) + zq\phi(x)]/kT)\,dx$$

will, therefore, be from the region just around $x = d/2$, or

$$\exp\left(\frac{-zqV}{2kT}\right) \cdot \int_{-r}^{d+r} \exp([W_e(x) + zq\phi(x)]/kT)\,dx \tag{61}$$

is approximately constant, independent of V. Eq. 61 was evaluated using numerical integral integration, assuming a linear variation in $\phi(x)$. The result is that

$$\exp\left(\frac{-zqV}{2kT}\right) \int_{-r}^{d+r} \exp([W_e(x) + zq\phi(x)]/kT)\,dx =$$

$$\exp[\omega(d) \cdot (qV/kT)^2] \cdot \int_{-r}^{d+r} \exp(W_e(x)/kT)\,dx, \tag{62}$$

for $V < 350$ mv. $\omega(d)$ is a parameter dependent on membrane thickness. $\omega(d)$ is tabulated in Table I (p. 813). For comparison, we have also tabulated $\omega(d)$ as a function of d, using the model of Neumcke and Läuger (38) and the approximation of Haydon and Hladky (18). According to the Eyring rate theory $\omega = 0$.

We thank A. Finkelstein, E. Greenbaum, E. Heyer, A. Mauro, and R. Muller for discussions and advice on the manuscript, and E. Bamberg and P. Läuger for a generous gift of dioleoylphosphatidylethanolamine.

O. S. Andersen is an Andrew W. Mellon Teacher-Scientist.

The present study was supported by National Institutes of Health grant GM 21342 to O. S. Andersen.

Received for publication 17 December 1974.

REFERENCES

1. ABRAMOWITZ, M., and I. A. STEGUN. 1965. Handbook of Mathematical Functions. Dover Publications, Inc., New York.
2. ARMSTRONG, C. M., and F. BEZANILLA. 1974. Charge movement associated with the opening and closing of the activation gates of the Na channels. *J. Gen. Physiol.* **63**:533.
3. BABAKOV, A. V., L. N. ERMISHKIN, and E. A. LIBERMAN. 1966. Influence of electric field on the capacity of phospholipid membranes. *Nature (Lond.).* **210**:953.
4. BENZ, R., G. STARK, K. JANKO, and P. LÄUGER. 1973. Valinomycin-mediated ion transport through neutral lipid membranes: influence of hydrocarbon chain length and temperature. *J. Membrane Biol.* **14**:339.
5. BLEANEY, B. I., and B. BLEANEY. 1965. Electricity and Magnetism. 2nd ed. Oxford University Press, London.

6. BOCKRIS, J. O. M., and A. K. N. REDDY. 1970. Modern Electrochemistry. Macdonald, London.
7. CIANI, S. M., G. EISENMAN, R. LAPRADE, and G. SZABO. 1973. Theoretical analysis of carrier mediated electrical properties of bilayer membranes. *In* Membranes, Vol. 2. George Eisenman, editor. Chap. 2. Marcel Dekker, New York.
8. COETZEE, J. F., and W. R. SHARPE. 1971. Solute-solvent interactions. VI. Specific interactions of tetraphenylarsonium, tetraphenylphosphonium and tetraphenylborate ions with water and other solvents. *J. Phys. Chem.* **75**:3141.
9. COGAN, U., M. SHINITZKY, G. WEBER, and T. NISHIDA. 1973. Microviscosity and order in the hydrocarbon region of phospholipid, and phospholipid-cholesterol dispersions determined with fluorescent probes. *Biochemistry.* **12**:521.
10. COX, B. G., and A. J. PARKER. 1972. Medium activity coefficient of silver cation between acetronitrile and water. *J. Am. Chem. Soc.* **94**:3674.
11. CRANK, J. 1956. Mathematics of Diffusion. Oxford University Press, London.
12. FINKELSTEIN, A., and A. CASS. 1968. Permeability and electrical properties of thin lipid membranes. *J. Gen. Physiol.* **52**:145.
13. FINKELSTEIN, A., and A. MAURO. 1963. Equivalent circuits as related to ionic systems. *Biophys. J.* **3**:215.
14. GRUNWALD, E., G. BAUGHMAN, and G. KOHNSTAM. 1960. The solvation of electrolytes in dioxane-water mixtures, as deduced from the effect of solvent change on the standard partial molar free energy. *J. Am. Chem. Soc.* **82**:5801.
15. GUGGENHEIM, E. A. 1929. The conceptions of electrical potential difference between two phases and the individual activity of ions. *J. Phys. Chem.* **33**:842.
16. GUGGENHEIM, E. A. 1930. On the conception of electrical potential difference between two phases II. *J. Phys. Chem.* **34**:1540.
17. HALL, J. E., C. A. MEAD, and G. SZABO. 1973. A barrier model for current flow in lipid bilayer membranes. *J. Membrane Biol.* **11**:75.
18. HAYDON, D. A., and S. B. HLADKY. 1972. Ion transport across thin lipid membranes: a critical discussion of mechanisms in selected systems. *Q. R. Biophys.* **5**:187.
19. HAYDON, D. A., and V. B. MYERS. 1973. Surface charge, surface dipoles and membrane conductance. *Biochim. Biophys. Acta.* **307**:429.
20. HLADKY, S. B. 1972. The steady-state theory of the carrier transport of ions. *J. Membrane Biol.* **10**:67.
21. HLADKY, S. B. 1974. The energy barriers to ion transport by nonactin across thin lipid membranes. *Biochim. Biophys. Acta.* **352**:71.
22. JOLICOEUR, C., and H. L. FRIEDMAN. 1971. Effects of hydrophobic interactions on dynamics in aqueous solutions studied by EPR. *Ber. Bunsen Ges.* **75**:248.
23. KETTERER, B., B. NEUMCKE, and P. LÄUGER. 1971. Transport mechanism of hydrophobic ions through lipid bilayer membranes. *J. Membrane Biol.* **5**:225.
24. KEYNES, R. D., and E. ROJAS. 1974. Kinetics and steady-state properties of the charged system controlling sodium conductance in the squid giant axon. *J. Physiol.* **239**:393.
25. KRAMERS, H. A. 1940. Brownian motion in a field of force and the diffusion model of chemical reactions. *Physica 7*, 284.
26. KRISHNAN, C. V., and H. L. FRIEDMAN. 1971. Solvation enthalpies of electrolytes in methanol and dimethylformamide. *J. Phys. Chem.* **75**:3606.
27. LAPRADE, R., S. M. CIANI, G. EISENMAN, and G. SZABO. 1974. The kinetics of carrier-mediated ion permeation in lipid bilayers and its theoretical interpretation. *In* Membranes, Vol. 3. G. Eisenman, editor. Marcel Dekker, Inc., New York. Chap. 2. In press.
28. LÄUGER, P., and G. STARK. 1970. Kinetics of carrier-mediated ion transport across lipid bilayer membranes. *Biochim. Biophys. Acta.* **211**:458.
29. LÄUGER, P., and B. NEUMCKE. 1973. Theoretical analysis of ion conductance in lipid bilayer membranes. *In* Membranes, Vol. 2. George Eisenman, editor. Marcel Dekker, Inc., New York. Chap. 1.
30. LE BLANC, O. H., JR. 1969. Tetraphenylborate conductance through lipid bilayer membranes. *Biochim. Biophys. Acta.* **193**:300.
31. LE BLANC, O. H., JR. 1970. Single ion conductances in lipid bilayers. *Biophys. Soc. Abstr.* 94*a*.
32. LIBERMAN, E. A., and V. P. TOPALY. 1969. Permeability of bimolecular phospholipid membranes for lipid soluble ions. *Biofizika.* **14**:452.

33. McLAUGHLIN, S. G. A., G. SZABO, G. EISENMAN, and S. M. CIANI. 1970. Surface charge and the conductance of phospholipid membranes. *Proc. Natl. Acad. Sci.* **67**:1268.
34. MUELLER, P., D. O. RUDIN, H. TI TIEN, and W. C. WESCOTT. 1963. Methods for the formation of single bimolecular lipid membranes in aqueous solution. *J. Phys. Chem.* **67**:534.
35. MULLER, R. U., and A. FINKELSTEIN. 1972. The effect of surface charge on the voltage-dependent conductance induced in thin lipid membranes by monazomycin. *J. Gen. Physiol.* **60**:285.
36. NEFEDOV, V. D., N. G. MOLCHANOVA, V. E. ZHURAVLEV, and T. I. BULYCHEVA. 1970. Cocrystallization of tetraphenylin labeled with tin-113, with tetraphenyl derivatives of Group IV elements. *Radiokhimiyia.* **12**:889. (*Chem. Abstr.* **74**:103655).
37. NEUMCKE, B. 1970. Diffusion polarization at lipid bilayer membranes. *Biophysik.* **7**:95.
38. NEUMCKE, B., and P. LÄUGER. 1969. Nonlinear electrical effects in lipid bilayer membranes. *Biophys. J.* **9**:1160.
39. PLANCK, M. 1890. Ueber die Erregung von Electricitat und Warme in Electrolyten. *Ann. Phys. Chem.* **2**:161.
40. PLANCK, M. 1890. Ueber die Potentialdifferenz zwischen zwei verdunnten Lösungen binarer Electrolyte. *Ann. Phys. Chem.* **40**:561.
41. RYAN, T. H., KORYTA, J., A. HOFANANOVA-MATEJKOVA, and M. BREZINA. 1974. Polarography of alkali metal ion complexes of macrotetrolides: complex ion size and stability. *Anal. Let.* **7**(5):335.
42. SHINITZKY, M., and Y. BARENHOLZ. 1974. Dynamics of the hydrocarbon layer in liposomes of lecithin and sphingomyelin containing dicetylphosphate. *J. Biol. Chem.* **249**:2652.
43. SIMON, W., and W. E. MORF. 1973. Alkali specificity of carrier antibiotics and their behavior in bulk membranes. *In* Membranes, Vol. 2. George Eisenman, editor. Marcel Dekker, Inc., New York. Chap. 4.
44. SKINNER, J. F., and R. M. FUOSS. 1964. Conductance of triisoamylbutylammonium and tetraphenylboride ions in water at 25°. *J. Phys. Chem.* **68**:1882.
45. SMYTHE, W. R. 1950. Static and Dynamic Electricity. 2nd edition. McGraw-Hill Book Company, Inc., New York. 121.
46. STARK, G., and R. BENZ. 1971. The transport of potassium through lipid bilayer membranes by the neutral carriers valinomycin and monactin. *J. Membrane Biol.* **5**:133.
47. STARK, G., B. KETTERER, R. BENZ, and P. LÄUGER. 1971. The rate constants of valinomycin-mediated ion transport through thin lipid membranes. *Biophys. J.* **11**:981.
48. SZABO, G., G. EISENMAN, S. G. A. McLAUGHLIN, and S. KRASNE. 1972. Ionic probes of membrane structures. *Ann. N.Y. Acad. Sci.* **195**:273.
49. TANFORD, C. 1973. The Hydrophobic Effect: Formation of Micelles and Biological Membranes. John Wiley & Sons, New York.
50. VAN DER ZIEL, A. 1968. Solid State Physical Electronics. 2nd edition Prentice-Hall, Inc., Englewood Cliffs, N.J.
51. WEAST, R. C., ed. 1972. Handbook of Chemistry and Physics. The Chemical Rubber Company, Cleveland, Ohio.
52. WHITE, S. A. 1970. A study of lipid bilayer membrane stability using precise measurements of specific capacitance. *Biophys. J.* **10**:1127.